University of Alberta

Towards a Better Understanding of Poly(*N*-isopropylacrylamide) Microgel-Based Etalons and their Continued Development in Diagnostics

by

Ian Heppner

A thesis submitted to the Faculty of Graduate Studies and Research
in partial fulfillment of the requirements for the degree of

Master of Science

Chemistry

Fall 2013
Edmonton, Alberta

To my parents

Abstract

Poly(N-isopropylacrylamide) (pNIPAm) microgel-based etalons are photonic materials that exhibit color based on temperature or other environmental stimuli. These materials provide a new and unique method for biosensing and other applications. Therefore it is important to understand these materials and to continue developing the materials in order to realise their full potential. This work examines the development of these materials in point-of-care (POC) diagnostics by exploring new and less expensive materials for etalon fabrication as well as examining the volume phase transition temperature of pNIPAm microgels and how it's affected by confinement in the etalon. It was found that the metal used in fabricating the device did not have a significant impact on the optical properties of the device. Additionally it was determined that the volume phase transition temperature (VPTT) of the microgels was not affected by their confinement in the device, and a VPTT was measured at methanol concentrations where no transition was previously observed.

ACKNOWLEDGEMENTS

First I would like to thank Dr. Serpe for giving me the opportunity to carry out these experiments in his laboratory. Dr. Serpe has always encouraged me to do my best and to consider different aspects of the work I did in the lab. Our discussions often led to further experiments and encouragement in my work. I would also like to thank the other members of the Serpe group, both past and present as well as all of my colleagues at U of A. Finally I would like to thank my parents, my brother, and my friend Rosina for their constant love and support throughout my entire stay with U of A.

TABLE OF CONTENTS

LIST OF FIGURES

LIST OF ABBREVIATIONS

pNIPAm – Poly(N-isopropylacrylamide)

UCST – Upper Critical Solution Temperature

LCST – Lower Critical Solution Temperature

VPTT – Volume Phase Transition Temperature

BIS – N,N'-methylenebisacrylamide

AAc – Acrylic Acid

APS – Ammonium Persulphate

λ – Wavelength

m – Peak Order

n – Refractive Index

d – Thickness of the Dielectric Material

θ – Angle of Incident Light

APBA – Aminophenylboronic Acid

POC – Point of Care

MeOH – Methanol

DI – Deionized Water

NIPAm – *N*-isopropylacrylamide

RCF – Relative Centrifugal Force

SUMMARY

This dissertation focuses on further understanding the fundamental properties and behavior of poly (*N*-isopropylacrylamide) (pNIPAm) microgel-based optical devices (etalons) the lab is developing; this understanding will facilitate further uses of the technology in the health and environmental sectors. Chapter 2 describes the fabrication of the pNIPAm microgel-based etalons using new and cheaper device components. This is to make the devices more economically feasible to use as disposable point of care diagnostic tools. Chapter 3 presents work conducted to understand how confinement of pNIPAm-based microgels between the etalon metal "mirrors" affects the microgels thermoresponsivity. Furthermore, we used the construct to investigate pNIPAm microgel cononsolvency -- a phenomenon that alters the microgels collapse transition temperature -- and compared the results to data obtained from microgels in solution. Chapter 4 contains conclusions and future directions of this work, including the further development in fabrication of the etalon device as well as examining pNIPAm microgel properties in additional environments.

CHAPTER 1

RESPONSIVE POLYMERS, POLY (N-ISOPROPYLACRYLAMIDE) MICROGELS AND POLY (N-ISOPROPYLACRYLAMIDE) MICROGEL-BASED ETALONS

1.1. Responsive Polymers

In recent years, responsive polymers have been examined for a number of applications including the removal of contaminants from water, the production of optical materials, and a number of analytical applications. A responsive polymer is a polymer that will undergo some physical and/or chemical change due to the application of stimulus. For example, a polymer can change conformation in response to the applied stimulus. The stimuli can be separated into three categories; physical stimuli, and chemical stimuli. Examples of physical stimuli are temperature, ionic strength, light, solvent, magnetic field, electric fields, and mechanical stress. Common examples of chemical stimuli are pH, the presence of certain analytes, and biomedical agents.

The response of the polymer to the environmental stimulus is a result of a change in the interactions between either the polymer chains or the polymer and the solvent. Chemical stimuli do this directly while physical stimuli alter the molecular interactions and cause some phase separation at certain points. The polymer's response can lead to certain advantageous properties that can be used for applications. They can be: a change in the permeability of the material, a change in size/shape of the material, or even a change in the optical properties of the polymer material. Some of the more recent applications of responsive

polymers involve the polymers responding to light, magnetic field, and detecting explosives[1-3] as well as a wide range of biosensing applications.[4, 5] Another recent application of responsive polymers is their use as a coating for silica beads in chromatography, providing strong hydrophobicity at elevated temperatures and being very stable due to their thermoresponsive nature.[6] In this way a coating can also be made that will change its physical properties based on stimuli such as temperature or pH, providing further separation of analytes. Responsive polymers can also change their physical properties based on conditions such as temperature so that they will bind to certain surfaces depending on the temperature, this opens up applications in adaptive biosensing within a biological system.[7] These application involve poly (*N*-isopropylacrylamide) (pNIPAm) which is one of the most heavily researched responsive polymers and is well known for its thermoresponsive nature and its transition temperature of approximately 32 °C.[8]

1.1.1. Temperature Responsive Polymers

Of particular interest here, and the most common type of stimuli responsive polymers, are polymers that are responsive to changes in temperature. Specifically here we will be talking about pNIPAm, which was first synthesised in the 1950's[9]. These polymers are widely researched due to the ease of altering the environment to affect a change in the system. When temperature responsive polymers are immersed in solvent they will either be in the same phase as the solvent or in separate phases, depending on the temperature of the system.[10, 11] The polymers will have either an upper critical solution temperature (UCST) or a

lower critical solution temperature (LCST). The UCST arises if the temperature needs to be decreased in order to affect a phase separation in the polymer solution, where as the LCST arises if the temperature needs to be increased to affect the phase separation in the polymer solution. This phase separation occurs due to a change in the free energy of the system. For example when considering a polymer solution with an LCST the solution will be stable and homogeneous while below this temperature due to hydrogen bonding between the polymer and solvent and a favourable free energy ($\Delta G < 0$). When the temperature is raised above the LCST the free energy will become positive due to the contribution from enthalpy now being greater than the contributions of entropy to the following equation:

$$\Delta G = \Delta H - T\Delta S \qquad (1)$$

When this occurs we see the interactions between polymer chains become more favourable than the interactions between polymer chain and solvent. This leads to the conformational change that is observed, an example of which can be seen in Figure 1-1.[12-14] In other words the polymer will become less soluble in the solvent as the temperature is increased.

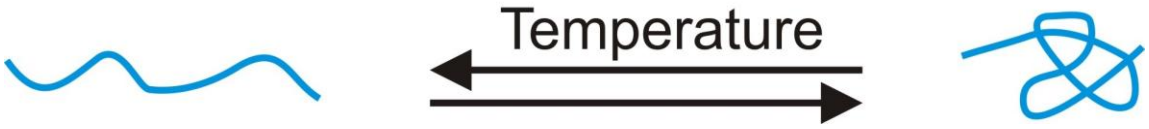

Figure 1-1. Random coil to globular conformational change of linear stimuli responsive polymer

The transition temperature observed for a temperature responsive polymer can be altered by the structure and chemical makeup of the polymer itself. The more hydrophilic a polymer is, for example if carboxylic acid or acrylamide groups are present, the stronger the interactions between polymer and solvent will be, and thus it will require more energy (higher temperature) to overcome these favourable interactions. Having more hydrophobic groups in the polymer such as t-butyl or isopropyl will have the opposite effect, having less favourable interactions between the polymer and solvent and so decreasing the temperature required to observe a conformational change[15]. The transition temperature will also be different depending on the solvent.

1.1.2. Temperature Responsive Hydrogels

A hydrogel is an interlinked polymer structure known as a network polymer. This structure arises from either a single chain being linked together at different points along the length of the chain, or from multiple chains coming together to form the interlinked structure. This will result in a three-dimensional structure of covalently bonded polymer chains, forming a large mesh structure. This can be done by physical crosslinking, a weak interaction that will degrade over time, or chemical crosslinking with a crosslinker during the synthesis of the polymer[16-20]. These network polymers can absorb a relatively large volume of solvent, due to their unique structure, while remaining undissolved in the solvent. Absorbing solvent results in a swollen state where the volume inside the structure is more solvent than polymer. Hydrogels are commonly classed by the size of the

gel, nanogels being the smallest followed by microgels and then macrogels. Of specific inters here are the microgels. Hydrogels have a wide variety of uses such as controlled drug delivery, contact lenses, synthetic membranes, photonic crystals, and other biomedical applications.[21-38]

When a hydrogel is made from temperature responsive polymer chains we can observe similar temperature responsiveness in the hydrogel as in a linear polymer chain of the same material. Because the polymer chains are linked together in the network polymer we no longer see a conformational change as the polymer chains are unable to break their bonds with other portions of the network polymer. Because of this there is no longer a macroscopic change in the structure, such as a conformational change, but rather a microscopic change as the individual portions of the polymer chains begin to contract.[39] This change leads to a change in volume as the polymers contracts but retain their overall shape due to the structure of the network polymer. This results in the structure expelling solvent as it becomes smaller in size, as seen in Figure 1.2. The temperature at which this occurs is called the volume phase transition temperature (VPTT) and can be altered in the same ways as the linear polymer, but now crosslink density is also a factor. The effects in the same when considering smaller sized hydrogels such as microgels.

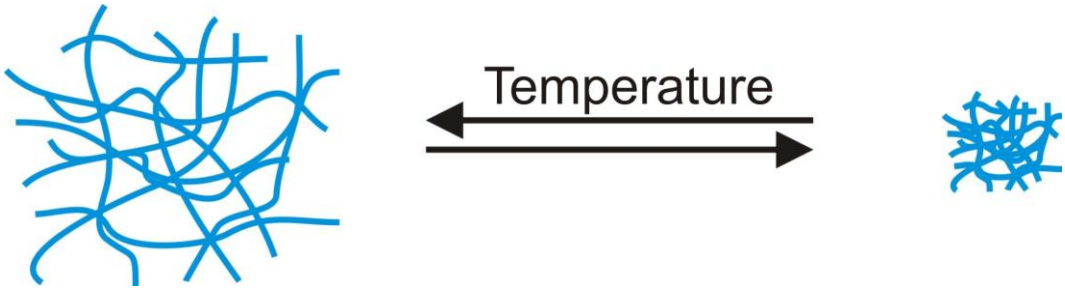

Figure 1-2. Deswelling of hydrogel made from stimuli responsive polymer

1.1.3. Poly (N-isopropylacrylamide) Based Microgels

Poly(*N*-isopropylacylamide) is possibly the most well known and thoroughly researched example of a stimuli responsive polymer. The polymer is well known for its coil to globular conformational change at approximately 32 °C in water, which makes it of great interest to investigation into possible biological applications. In effect linear pNIPAm will be soluble in water under 32 °C in a random coil conformation. When the solution is heated above this temperature the pNIPAm will collapse in to a globular conformation and will no longer be soluble in water, causing the solution to become cloudy as the polymer precipitates from solution. The structure of pNIPAm can be seen in Figure 1-3, pNIPAm has a hydrophilic amide group and a hydrophobic isopropyl group giving it this LCST which is in an ideal range for work with biomedical applications. pNIPAm is well known for its reversible transition between a random coil conformation and globular conformation when the temperature approaches the LCST. It is because of the temperature of the transition and the reversible nature of the conformational change that this polymer is so widely studied. When synthesised with a

crosslinker such as N,N'-methylenebisacrylamide (BIS) pNIPAm can form a colloidally stable microgel with the same temperature responsive characteristics as the linear polymer. These microgels will now expel the water of salvation at the VPTT at 32 °C. Of interest also is the ease with which the polymer can be functionalised with various groups. The pNIPAm can be synthesised with co-monomers such as acrylic acid (AAc) to give additional functionality by making the polymer not only temperature responsive but also pH responsive. The AAc also provide a site to be further functionalised and provide additional responsivity to analytes and biomarkers.

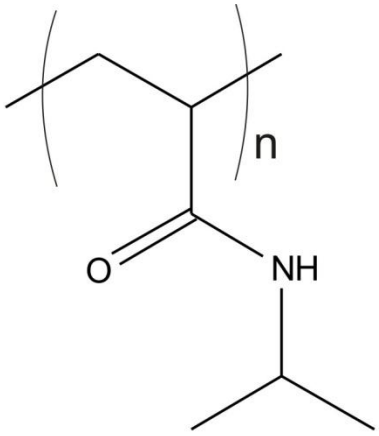

Figure 1-3. Structure of poly(*N*-isopropylacrylamide), n being the number of repeating monomer units.

There has been much work done to understand pNIPAm microgels and their thermoresponsive properties and applications. One such example is the work of Richtering where the VPTT of pNIPAm microgels is determined using

dynamic light scattering and small angle neutron scattering and comparing these results with previous work by Winnick and Tirrell for the LCST of linear pNIPAm.[8, 10, 40, 41] It was found that the transition temperatures were very similar between pNIPAm in linear and microgel form. In addition there has been work done by Lyon to fabricate colloidal crystals using temperature and pH responsive pNIPAm microgels.[21, 22, 25] This gives a bright iridescent color that can change depending on the temperature or pH of the environment. An example of potential applications by Lyon is their investigation in using pNIPAm copolymers functionalised with biotin so that the binding of avidin and anti-biotin can be detected using optical spectroscopy, this process being reversible.[36] In addition to functionalising the pNIPAm polymers to give additional responsivity to the polymer, Kawaguchi has reported on using core/shell microgel structures to immobilise material in the core of the microgel.[30, 31] This method opens up a wide range of possibilities including magnetic, optical, and biomedical applications. One such application is the removal of contaminants from water by absorption[26, 27]. In addition there has been work done in using pNIPAm based microgels optical devices that are optically tunable due to their responsiveness to temperature.[21, 25, 31] Optical devices made using pNIPAm based microgels include three-dimensional photonic crystals and Fabry–Pérot interferometers.[42, 43]

1.1.4. Synthesis

Common techniques for the synthesis of responsive polymers are anionic polymerization and free radical polymerization. The synthesis of hydrogels is

accomplished by adding additional cross-linker species to these reactions. A cross-linker will bond to more than one polymer chain in solution creating a network polymer instead of a linear polymer. In anionic polymerization a negatively charged species, such as a carbanion, is introduced into solution with the desired monomers. The negatively charged species will react with the monomer at a double bond creating a covalent bond between the two species. The negative charge will now be on the monomer and can react with additional monomers to continue chain propagation.

The second type of polymerization, and more relevant to this work, is the free radical polymerization. In this polymerization a free radical is created in solution with the desired monomers, often by using a species with a weak single bond that can be broken at elevated temperatures to create free radicals. An example of such a reagent is ammonium persulfate (APS). The free radical can then react with the monomer and, either by forming a covalent bond with the monomer or by removing a hydrogen, can cause the monomer to become a free radical. This new free radical monomer can then react with additional monomers forming covalent bonds and remaining a free radical to further propagate the polymerization.

1.1.5. Applications

Due to the ability to make pNIPAm responsive to a wide variety of stimuli they have potential applications for sensing or possibly the mechanical force

produced by the polymer response. Some of the potential uses of pNIPAm and pNIPAm based microgels are biosensing, controlled drug delivery, and use in biomaterials. A recent investigation into the potential uses of pNIPAm is the removal of contaminants from water, which has seen work into the use of pNIPAm and pNIPAm copolymers to remove organic molecules and dyes from solution.[26, 27] There has also been work done in using pNIPAm microgels in creating photonic materials such as basic interferometers that can respond to various stimuli.[42, 44]

1.2. Poly(*N*-isopropylacrylamide) Microgel Based Etalons

A Fabry–Pérot interferometer, also known as an etalon, is a one dimensional optical material that emits a certain wavelength of light determined by the resonance of light through a cavity between two reflective surfaces.[45, 46] Recently these optical devices have been made using pNIPAm based microgels to actively tune the distance between these two reflective surfaces, dynamically changing the wavelength of light that is emitted. These tunable etalons have shown promise in a number of applications such as glucose sensing.[47]

1.2.1. pNIPAm Microgel Based Etalon

The Fabry–Pérot interferometer is in form two semi-transparent, reflective surfaces with a dielectric material in between. When light strikes the device it is reflected and refracted through the reflective material, the refracted light will then

undergo constructive interference if the light is in phase and destructive interference if the light is out of phase resulting in characteristic reflectance spectra of maximum and minimums at different wavelengths. This behaviour is shown in Figure 1-6 and is governed by the equation:

$$\lambda m = 2nd \cos\theta \qquad (2)$$

Here λ is the wavelength of reflected light, m is the order of the peak, n is the refractive index of the dielectric material, d is the distance between the two reflective surfaces or the thickness of the dielectric material, and θ is the angle of incident light.[43]

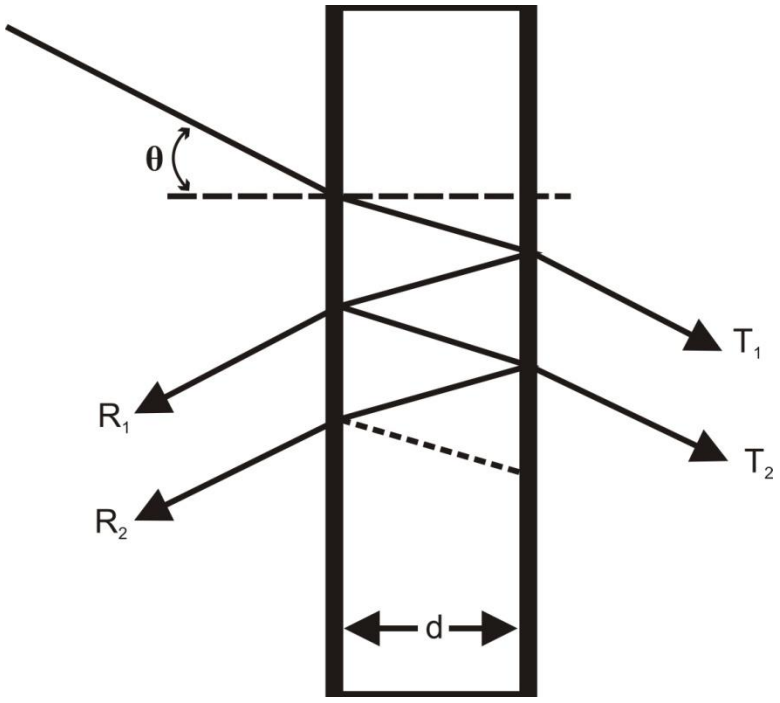

Figure 1-4. Light interacting with Fabry–Pérot interferometer

Recently these etalons have been fabricated using pNIPAm based microgels that are approximately 1.5 μm in size as the dielectric material showing color when immersed in water and allowing for the distance between the two reflective surfaces to be dynamically tuned. This allows for the color of reflected light to be changed, when the device is immersed in water, by raising the temperature of the system. This is due to the dependence of the peak wavelength on the distance between the two reflective surfaces or thickness of the dielectric material. With pNIPAm as the dielectric material this distance will decrease as the temperature is increased and the microgels collapse. In the equation the distance is directly related to the wavelength and so as the distance decreases so will the peak wavelength of reflected light, changing the observed color of the device. If the pNIPAm microgels contain co-monomers or further functionalised groups the device can respond to additional stimuli such as pH or even the presence of glucose.

1.2.2. Fabrication

The pNIPAm microgel-based etalons are fabricated using Au as the reflective, semi transparent surfaces. First a layer of Cr/Au is deposited onto a glass substrate that is 2.5 cm by 2.5 cm. Cr is used so that the Au will adhere to the glass substrate. The pNIPAm based microgels are then deposited on to the Cr/Au layer using a "paint-on" procedure developed specifically for this. A final layer of Cr/Au is then deposited over the microgels to complete this structure. A schematic of this structure can be seen in Figure 1-7.[42, 44]

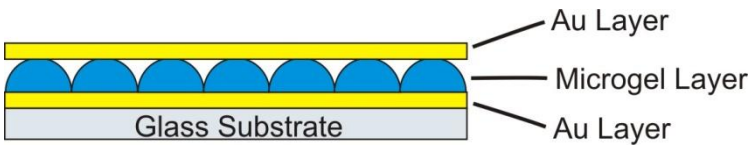

Figure 1-5. Rendering of pNIPAm microgel-based etalon

1.2.3. Applications

The pNIPAm microgel-based etalons have been shown to change color as the temperature or pH of the solvating liquid is altered. An example of this change can be seen in Figure 1-6 along with reflectance spectra of a pNIPAm microgel-based etalon with the same peak marked at two temperatures.

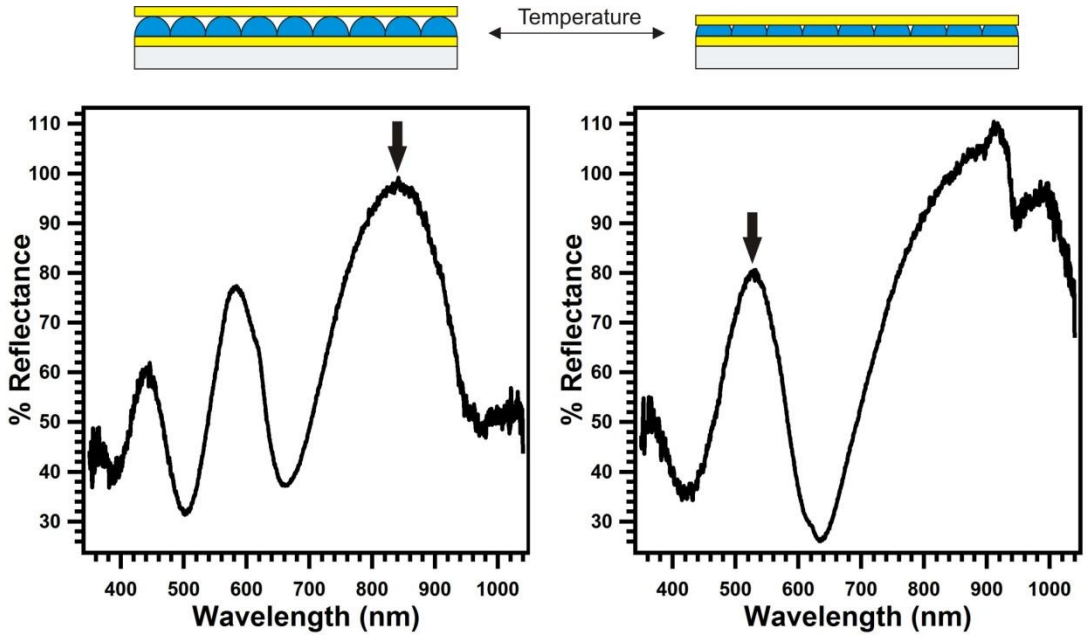

Figure 1-6. Rendering of pNIPAm microgel-based etalon as temperature is increased with corresponding reflectance spectra below and peak of order 2 marked

In addition to this color tunability there are a number of potential applications for pNIPAm microgel-based etalons including those that have previously been explored. In one publication the microgels used to fabricate the etalon were co-polymerized with AAc and functionalized with aminophenylboronic acid (APBA) allowing the microgels to be glucose sensitive[47]. In this way there was not only a spectral change in wavelength when glucose was added to the solution containing the device, but a visual color change was also observed. From this proof-of-concept it is apparent the potential applications of the device in biosensing, with the possibility of visual color change indicating the results. For example Figure 1-7 showing one possible mechanic for DNA sensing. Furthermore there has been work done in testing the pH and temperature response of spatially isolated regions of an etalon.[48, 49] This indicates that an etalon device can be fabricated with multiple test areas on a single device, possible sensing for multiple small molecules simultaneously. In addition to biosensing the device has recently shown promise in detecting polyelectrolytes by size and charge.[50, 51] The charge selectivity arises from the presence of pH responsive co-monomer in the microgel and being at a pH that gives an overall charge to the microgels allowing the opposite charge to be detected. The size exclusion arises from pores in the Au layer, the size of which can be controlled by changing the thickness of the top Au layer.

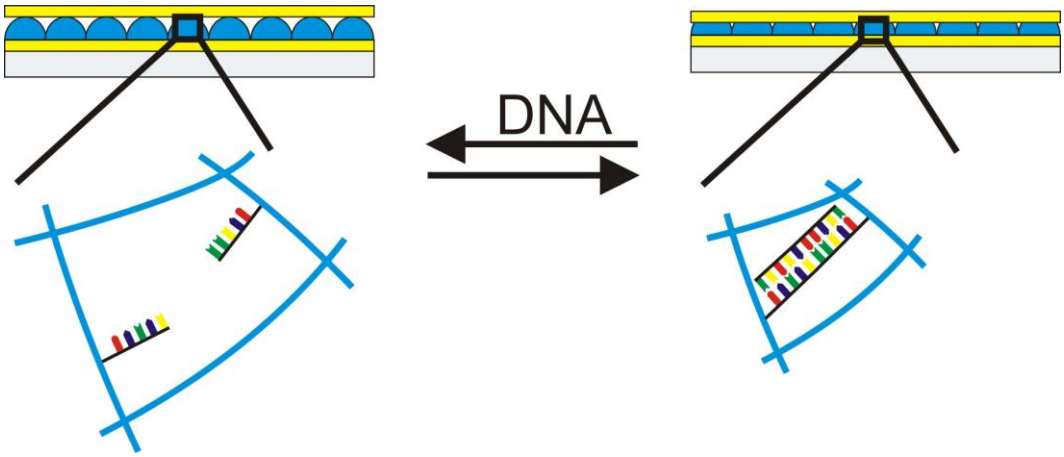

Figure 1-7. Schematic of potential DNA sensing mechanic

1.3. Point of Care Diagnostics

There is a large demand in developing countries for diagnostic devices that can be used away from a hospital or laboratory setting. This is due to a large part of the population being unable to easily access a medical facility or not having trained personnel or proper equipment to properly diagnose disease in these areas. This can result in not treating the problem, or even treating something not afflicting the patient possibly leading to a worsening of the symptoms or even death. Point of care (POC) diagnostic devices attempt to circumvent this barrier in service by providing a device that can be carried to the patient and used on site. Ideally these devices would not require facilities that may not be available in some areas, such as running water or electricity, and would be robust, being able to operate in potentially harsh conditions. The devices should be simple enough that they could be used with little to no training to minimize contamination and still give accurate results. Lastly the device should be inexpensive to use and fabricate in order to make it more available in all regions that need treatment.[52]

Poly(N-isopropylacrylamide) microgel-based etalons could be ideal for point of care diagnostics as they are simple to use, require only a small amount of water, and can give a visual readout for diagnostic results. One downside to the use of these devices in POC diagnostics is the actual materials the etalon devices are made from. The microgels and glass used to fabricate the etalons a relatively inexpensive but the reflective surfaces are made from the precious metal Au, and so could be expensive to mass produce. It is important to investigate other materials that could be used to fabricate the devices in order to realise their full potential as a POC diagnostic device.

1.4. Research Objectives

Fabry–Pérot interferometers have been fabricated using pNIPAm based microgels. These devices inherit the temperature responsive nature of the pNIPAm based microgels, allowing the color of the device to be tuned by increasing or decreasing the temperature of the solution they are immersed in. Though these devices have been shown to work for a number of applications, such as the detection of glucose, they require specific resources and equipment to fabricate and currently have not been fabricated on a large scale. It is important for these devices to be more readily manufactured and, combined with their ease of use; they could make ideal point-of-care diagnostic devices. There is a high demand for such devices due to a large portion of the world not having access to modern diagnostic and medical facilities. It is also important to understand these devices and how the properties of the responsive polymer may change when bound to such a device, and how the device itself can lead to a better

understanding of these properties. The purpose of this chapter is to give a brief introduction to responsive polymers, specifically pNIPAm, and the etalon device fabricated using pNIPAm based microgels

With this in mind the main purpose of this work is to investigate alternate, less expensive material that can be used to fabricate the etalons while providing similar sensitivity and visual color change when the etalon device is immersed in water and the temperature modulated to initiate a response. In addition the focus is on expanding the current understanding of the pNIPAm microgel-based etalons devices by examining what effect, if any, the confinement of the microgels in the device has on the VPTT of the microgels. This is done using cononsolvency of pNIPAm in water/methanol solutions to examine multiple VPTTs and compare between microgels in solution and microgels confined in an etalon device.

Chapter 2

Poly (*N*-isopropylacrylamide) Microgel - Based Etalons Constructed from Various Metal Layers

2.1. Introduction[1]

Diagnosing and treating ill patients in rural regions of developing countries is particularly difficult. This is due, in part, to the difficulty of patients physically getting to a hospital setting where a lab - based diagnostic test can be performed and proper treatment can be administered. If an ill patient cannot get to a hospital setting for diagnosis, they are often treated based on clinical signs of disease. This diagnosis has a high probability of being inaccurate, and the patient being treated for a disease they do not have. This situation, often referred to as disease overtreatment, is very problematic for numerous reasons and can ultimately lead to patient death. One reason for patient death is the fact that they are not being treated for the specific disease that is resulting in their observed clinical symptoms. Therefore, to decrease the barrier to receiving a correct diagnosis, devices must be made such that they can be brought to the patient, as opposed to the patient being transported to get a diagnosis. To be useful, the diagnostic devices (often referred to as point of care -- POC -- diagnostics) should not only be accurate, but must be capable of operating in harsh environments, with little to no infrastructure. Ideally, the diagnostic device should be able to operate with no running water or electricity, and in environments with extreme

[1] *A version of this chapter has been published. Heppner, I.; Serpe, M., Poly (N-isopropylacrylamide) microgel-based etalons constructed from various metal layers. Colloid Polym. Sci.* ***2013****, 1-6.*

heat and other deleterious environmental factors. Furthermore, the diagnostic device should be easy to operate, such that no extensive training of personnel is needed to run the test. The sample introduction should be straightforward to minimize contamination, and the result of the test should be capable of being determined in an unambiguous manner without the use of expensive equipment. Finally, the test should be able to be performed on whole blood or urine with minimal cost.

There have been a considerable number of advances related to POC diagnostics.[34, 47, 52, 54-60] Of particular interest to the work here are diagnostic devices that exhibit visual color.[33, 34, 47, 54, 56, 58, 61-64] At the core of these devices are often photonic materials, which are structures composed of at least two materials with different refractive indices arranged in a periodic fashion.[21, 65-68] These periodic structures interact with light, yielding constructive and destructive interference, which ultimately yields visual color. One such example of a photonic material is the Fabry—Pérot interferometer (etalon), which consists of two semi-transparent reflective surfaces deposited on two sides of a planar dielectric material.[45] Similar to traditional photonic materials, these devices exhibit color due to constructive and destructive interference of light resonating in the dielectric cavity between the metal layers.

We have recently reported on color tunable etalons using thermoresponsive poly (N-isopropylacrylamide) (pNIPAm)-based microgels.[42, 43, 47-49, 55] The devices are fabricated by "painting" the pNIPAm-based microgels onto Au coated glass surfaces.[42] Using this "painting" process, a concentrated

solution of microgels is simply spread onto a Au coated glass substrate followed by drying and copious rinsing with water. This procedure results in a robust, "monolithic" microgel layer on the Au.[42, 43, 47, 48, 55] Subsequently, another layer of Au is deposited onto the microgel layer. A schematic of the etalon's structure can be seen in Figure 2-1. In water, at T < ~ 32 °C -- the volume phase transition (VPT) for pNIPAm[8, 9, 32, 38-40, 69-72] -- the pNIPAm microgel layer of the etalon swells, resulting in a given dielectric thickness that yields visible color. We have shown that the device's color changes upon increasing the solution temperature to > ~ 32 °C. This is because the microgels collapse, bringing the reflective surfaces closer to one another. We have exploited this phenomenon for temperature, pH and glucose sensing.[42, 47, 49]

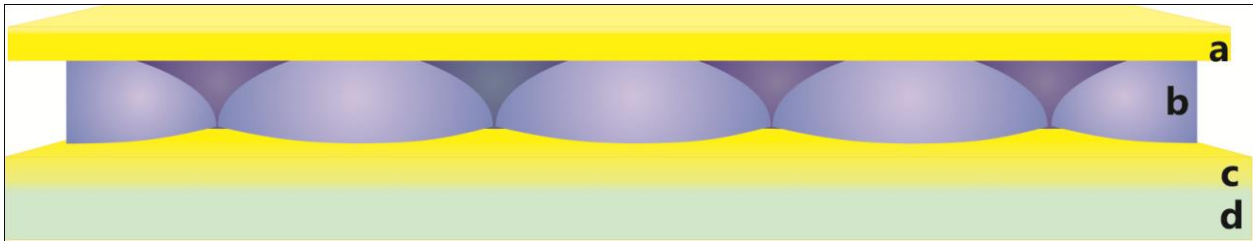

Figure 2-1. (a) A cartoon depiction of an etalon where (a) and (c) are reflective surfaces, (b) is the microgel dielectric, and (d) if the glass substrate base.

In addition to observing visual color changes, reflectance spectra from the devices can also be collected. As can be seen in Figure 2-4(b), the spectra exhibit multiple peaks, which all contribute to the observed color.[43] The position and number of peaks in the reflectance spectra can be described from equation (1):

$$\lambda m = 2nd \cos\theta \quad (1)$$

Where n is the refractive index of the dielectric material, d is the dielectric thickness, m is the peak order, and θ is the angle of incident light. From the equation it is clear that the position of the reflectance peaks (λ_{max}) is directly related to the refractive index of the dielectric material and the distance between the reflective surfaces.

These etalons have shown promise for sensing applications. Specifically, we are currently designing microgel-based etalons for detecting DNA, carbohydrates, and proteins in biological samples. Before these devices can be implemented, a number of questions must be answered, and barriers overcome. One specific barrier is making the devices out of less expensive materials, e.g., making etalons from metals other than Au. Despite the fact that etalon's Au layers only have a thickness of 15 nm, Au is a precious metal and if etalons are fabricated on a large scale the cost can become significant. Here, we evaluate the possibility of fabricating pNIPAm microgel-based etalons using metals such as: Cu, Al, Ti, and Ni. At the time of writing these metals are 3.33, 0.86, 23944, and 6.82 USD/lb and Au is 22352 USD/lb for a comparison of fabrication consts. The focus of the paper is on the function of the devices, and not necessarily a detailed description of the optical properties of the devices constructed from the various

metals. The results indicate that the layers surrounding the microgels need only be reflective, and do not necessarily need to be Au.

2.2. Materials and Methods

Materials: *N*-Isopropylacrylamide (NIPAm) was purchased from TCI (Portland, Oregon) and purified by recrystallization from hexanes (ACS reagent grade, EMD, Gibbstown, NJ. *N,N'*-methylenebisacrylamide (BIS, 99%) and ammonium persulfate (APS, 98% +) were obtained from Sigma-Aldrich (Oakville, Ontario) and were used as received. Methanol (MeOH, 99.8%) and tetrahydrofuran (THF, 99.0%) were purchased from Caledon Chemicals (Georgetown, Ontario) and were used as received. All deionized (DI) water was filtered through a Milli-Q Plus System (Millipore, Billerica, MA) to a resistivity of 18.2 MΩ·cm. Cr/Au annealing was done in a Thermolyne muffle furnace from Thermo Fisher Scientific (Ottawa, Ontario). Anhydrous ethanol was obtained from Commercial Alcohols (Brampton, Ontario). Fisher's Finest glass cover slips, 25 x 25 mm, were purchased from Fisher Scientific (Ottawa, Ontario). Cr and Au (99.999%) were purchased from ESPI (Ashland, OR). Al (99.00%), Ni (99.995%), Ti (99.995%), and Cu (99.99%) were purchased from Kurt J. Lesker Company (Clairton, PA).

Microgel Synthesis: Poly (*N*-isopropylacrylamide) based microgels were synthesised by a surfactant free, free radical precipitation polymerization reaction as previously described.[42] The total monomer concentration was 140 mM, and was 95% N-isopropylacrylamide (NIPAm) and 5% N,N'-methylenebisacrylamide (BIS, crosslinker). The monomer, NIPAm (13.3 mmol) and crosslinker, BIS (0.7

mmol) were dissolved in 80 mL of deionized water in a 150 mL beaker while being stirred. The mixture was then filtered, through a 0.2 µm filter on a 20 mL syringe, into a 250 mL round bottom flask. The beaker was then rinsed with an additional 19 mL of deionized water, which was then also filtered into the round bottom flask. The round bottom flask was then fitted with a temperature probe, a condenser, and a N_2 needle inlet. The reaction mixture was heated to 65 °C at a rate of 30 °C per hour, while being purged with N_2 and stirred at a rate of 450 rpm. Once a constant temperature was reached (~90 minutes) the N_2 needle was removed from the solution, while keeping a N_2 atmosphere, and APS (0.2 mmol) dissolved in 1 mL of deionized water was added to the reaction mixture to initiate the reaction. The reaction was then allowed to proceed for 4 hours, then removed from heat and allowed to cool to room temperature overnight. This procedure is summarised in Figure 2-2. Once at room temperature, aggregates were removed by filtering the polymer mixture through Whatman #1 qualitative filter paper (Fisher Scientific, Ottawa, Ontario) and rinsing with deionized water. The solution was then transferred to centrifuge tubes and centrifuged at ~8400 relative centrifugal force (RCF) at 22 °C for 30 minutes until the microgels formed a concentrated pellet at the bottom of the tubes. The supernatant was then removed and the microgels were resuspended in 12 mL of deionized water. This was done a total of 6 times to remove left over monomer and polymer chains from the microgel mixture.

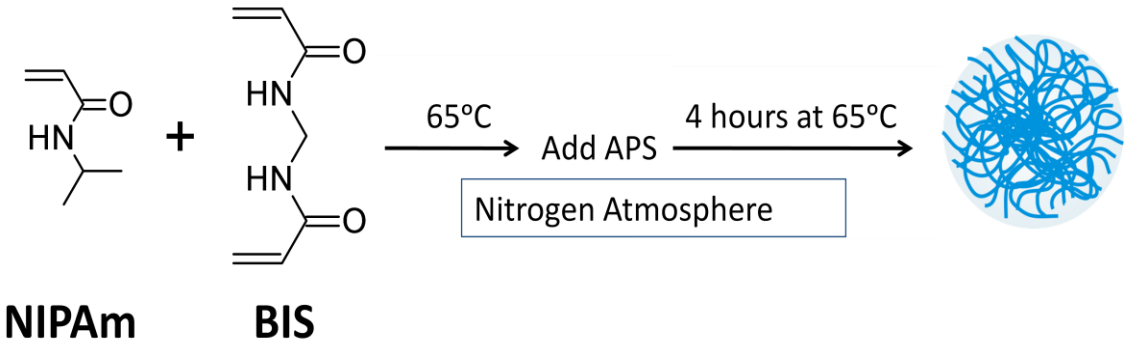

Figure 2-2. Microgel synthesis.

Etalon fabrication: The Cr/Au layers were deposited using a Torr International Inc. model THEUPG thermal evaporation system (New Windsor, NY) and all other metals (Al, Ni, Cu, and Ti) were deposited using a custom built medium throw Johnson Ultravac (JUV) electron beam evaporation system (Burlington, Ontario) that was made to NORTEL (Mississauga, Ontario) specifications. For each sample a 25 x 25 mm glass substrate was washed with ethanol and dried under N_2 before metal deposition under vacuum (low 10^{-6} torr range). The substrates using Cr/Au as a base layer were annealed in a Thermo Scientific thermolyne oven from Fisher (Waltham, MA) at 250 °C for 3 hours before use, and is the only metal layer using a Cr adhesion layer. Microgels were then applied directly to the metal layer using the previously mentioned painting protocol.[42]

Briefly, microgel solutions were centrifuged at ~8400 relative centrifugal force (RCF) for 60 minutes at 22 °C to form a concentrated microgel pellet at the bottom of the centrifuge tube. The metal substrates were then rinsed with ethanol

and dried under N_2 before being placed on a hot plate at 35 °C. Once on the hot plate, 40 µL of the concentrated microgels was pipetted on to the substrate and spread evenly using the side of the micropipette tip being careful not to scratch the metal layer. The substrate was then rotated and the microgels were spread more as they began to dry. Once evenly covered, the microgels were allowed to dry for 2 hours and then rinsed copiously with DI water until all excess microgels (microgels not directly adhered to the metal layer) were removed. The substrates were subsequently soaked overnight in deionized water or, in the case of Al and Cu, methanol at 35 °C. After soaking overnight, the substrates were rinsed once more with DI water and dried with N_2 gas, then coated with a second metal layer using the described method.

Reflectance Spectroscopy: Reflectance spectra were collected using a USB2000+ spectrophotometer, an HL-2000-FHSA halogen light source, and a R400-7-VIS-NIR optical fibre reflectance probe from Ocean Optics (Dunedin, Florida). All data was recorded using Spectra Suite software from Ocean Optics. The reflectance was measured in the range of 350 to 1039 nm and was done in a custom made chamber for sample positioning and temperature control. For temperature ramp experiments, the etalons were placed in the chamber and the temperature was raised from 25 °C to 40 °C in 3 °C increments, the spectrum being recorded at each temperature once the reflectance spectra were stable. The experimental apparatus used can be seen in Figure 2-3.

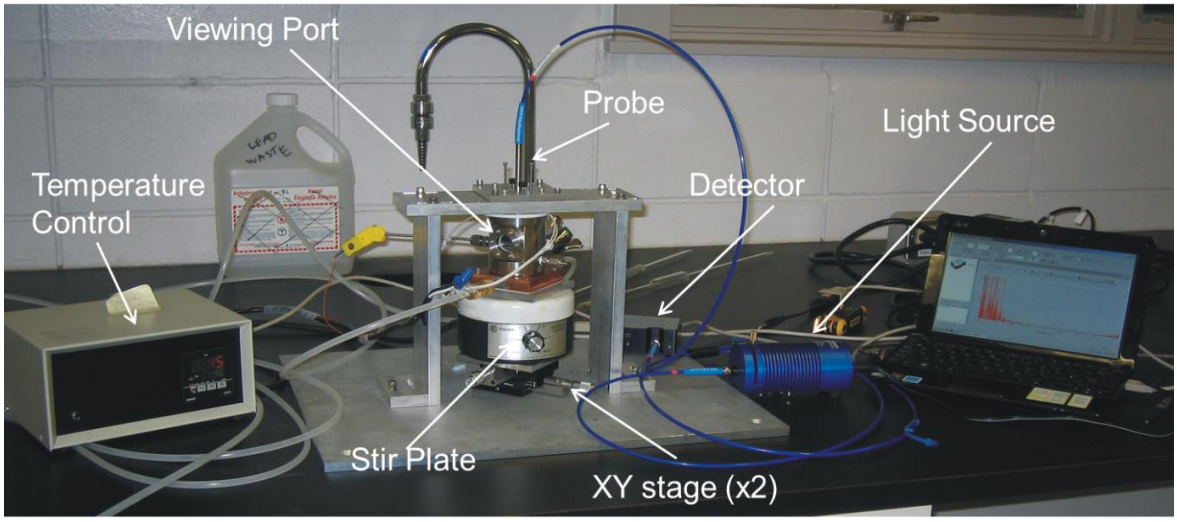

Figure 2-3. Reflectance spectrometer used in experiments.

Microscopy: Microscopy images were taken using an Olympus IX71 inverted microscope (Markham, Ontario) with a 100x oil-immersion objective, 10x eyepiece, differential interference contrast (DIC) optics, and Andor Technology iXon+ camera (Belfast Ireland). To capture images, Andor SOLIS v4.15.3000.0 software was used. For scale bars a PYSER-SGI scale grating (50 x 2 microns) from Edmunds Industrial Optics (Barrington, New Jersey) was used.

2.3. Results and Discussion

As stated above, less expensive etalon fabrication materials are required to make them a viable option for point-of-care diagnostics. Here, we evaluate the effect that different metal layers have on the etalon's optical properties and function. To this end a number of different metals were selected and used in the fabrication of etalons and the reflectance spectra and thermal response were analyzed. Specifically, we used Au, Ti, Ni, Al, and Cu. In all cases, the glass cover slips were coated with 15 nm of the respective metals, with the exception of

Al, which was coated to a thickness of 10 nm due to its high reflectivity. The microgel layers were then added to these metal-coated substrates, as detailed in the experimental. Following the microgel layer deposition, the resulting slides were subsequently coated with a second layer of metal in such a way as to give etalon samples with 16 different metal combinations possible (excluding Au layers). Reference etalons were also fabricated using Au as both metal layers.

In order to fabricate etalons, a "monolayer" of microgels needs to be formed on the metal layer deposited on the glass substrate. The microgels that make up the monolayer should also be "jammed" or “close packed”. That is, there should be no space between the microgels on the metal layer effectively forming a monolithic microgel layer. If this is not the case, an etalon will not be formed.[42] The quality of the resulting pNIPAm microgel-based layer can be determined using standard optical microscopy, as seen in Figure 2-4 (a) for the standard Au-based etalons. As can be seen from the figure, a "jammed" layer of microgels is obtained. The reflectance spectrum of the resulting etalon in water is shown in Figure 2-4 (b), and reveals a multipeak spectrum that is characteristic of a Au-based etalon. This etalon will serve as our "reference". That is, we strive to make etalons from different metal layers, which exhibit the same optical properties as the Au-based assemblies.

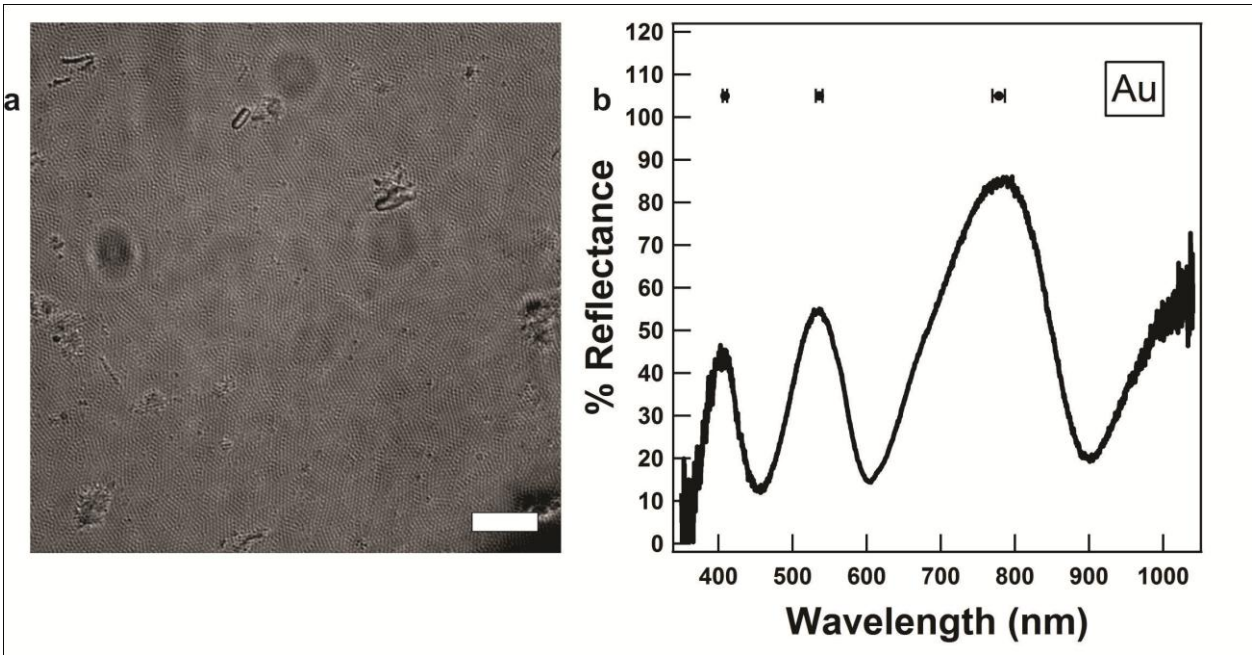

Figure 2-4. (a) DIC microscopy image of etalon with 2 nm Cr and 15 nm Au for top and bottom reflective layer, the scale bar is 10 μm. (b) Reflectance spectrum of etalon using 2 nm Cr and 15 nm Au for both top and bottom reflective layer. The marker above each peak depicts the average peak position for 4 spectra collected on 4 random spots on the etalon, the error bars showing the standard deviation associated with the peak position.

Figures 2-5 (a), 2-6 (a), 2-7 (a), and 2-8 (a) shows DIC microscopy images of etalons fabricated using Al, Cu, Ni, and Ti. As can be seen in each image, the painting protocol yielded a "close packed" or "jammed" microgel layer on Al, Cu, Ni, and Ti. Additionally, as can be seen in Figures 2-9 (a), 2-10 (a), 2-11 (a), and 2-12 (a), when a subsequent metal layer was deposited onto the resulting microgel layer, the expected multipeak spectra from etalons was observed. In each case,

regardless of the metal, a jammed microgel layer could be obtained, which yielded the expected (and desired) optical properties. We would like to point out here that there are obvious differences in the position/intensity of the peaks in the spectra obtained for the various etalons. We attribute these differences to the reflectivity variations for the different metals that make up the etalons. This could be adjusted by careful modulation of the thickness of the metal layers during metal evaporation. Another possible reason for the differences is due to the microgel layer structure. With each metal, there will be slightly different adhesion forces holding the microgels to the metal layer deposited on the glass, possibly due to metal oxides interacting with the microgels using different mechanisms. Therefore, slightly different microgel layer thicknesses could result from depositing the same microgels on various metal layers. Regardless, the devices exhibit the expected optical properties. Furthermore, for the etalons above, we deposited the same metal for both of the etalon's mirrors, although this does not have to be the case. For example, a different metal can be used for the top and bottom layer. The figures and the resulting reflectance spectra for these samples can be seen in Figures 2-5 to 2-12.

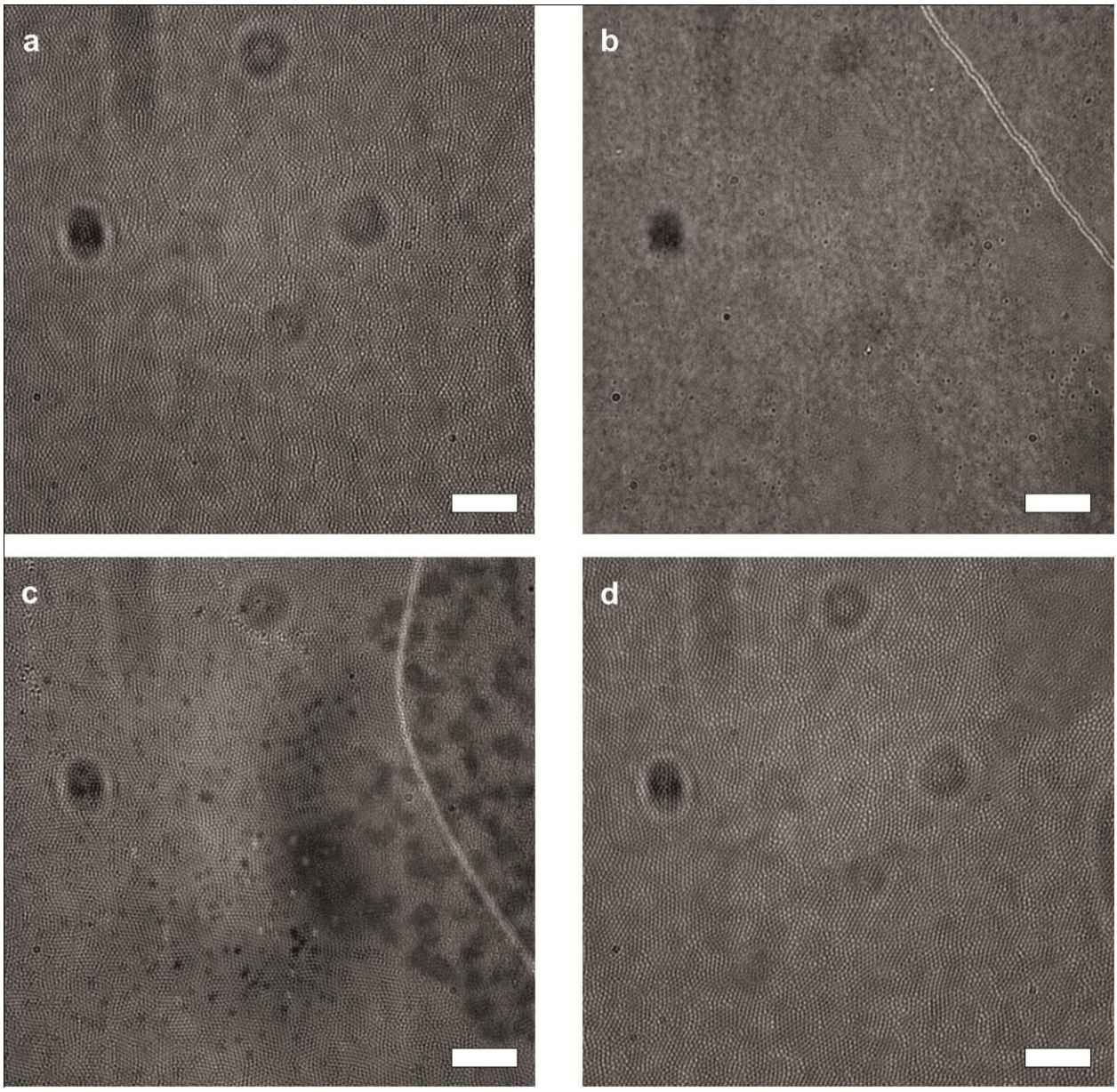

Figure 2-5. DIC microscopy images of an etalon fabricated using Al for the bottom reflective layer and (a) Al, (b) Cu, (c) Ni, or (d) Ti for the top layers. In each image the scale bar is 10 μm.

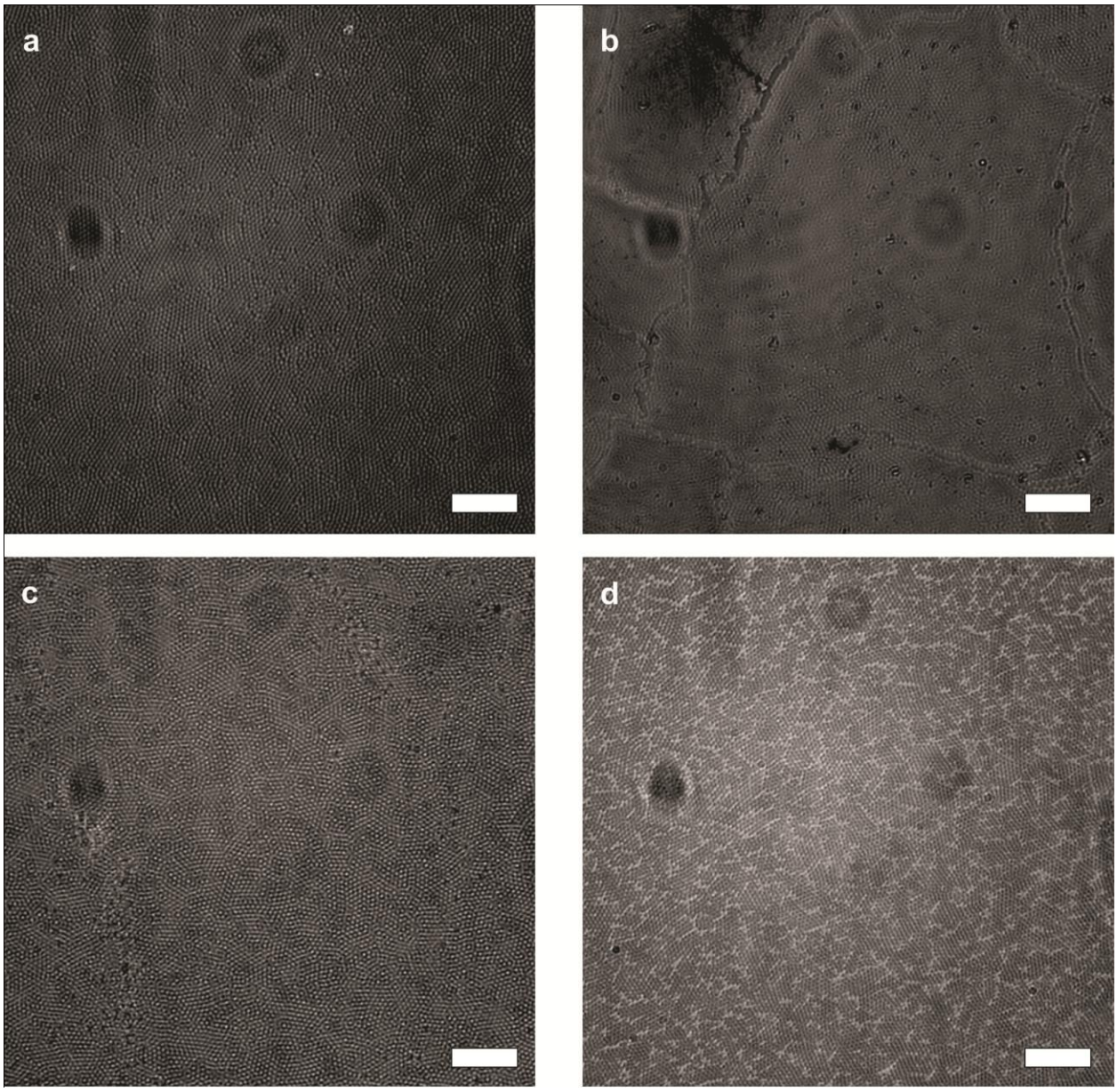

Figure 2-6. DIC microscopy images of an etalon fabricated using Cu for the bottom reflective layer and (a) Al, (b) Cu, (c) Ni, or (d) Ti for the top layers. In each image the scale bar is 10 μm.

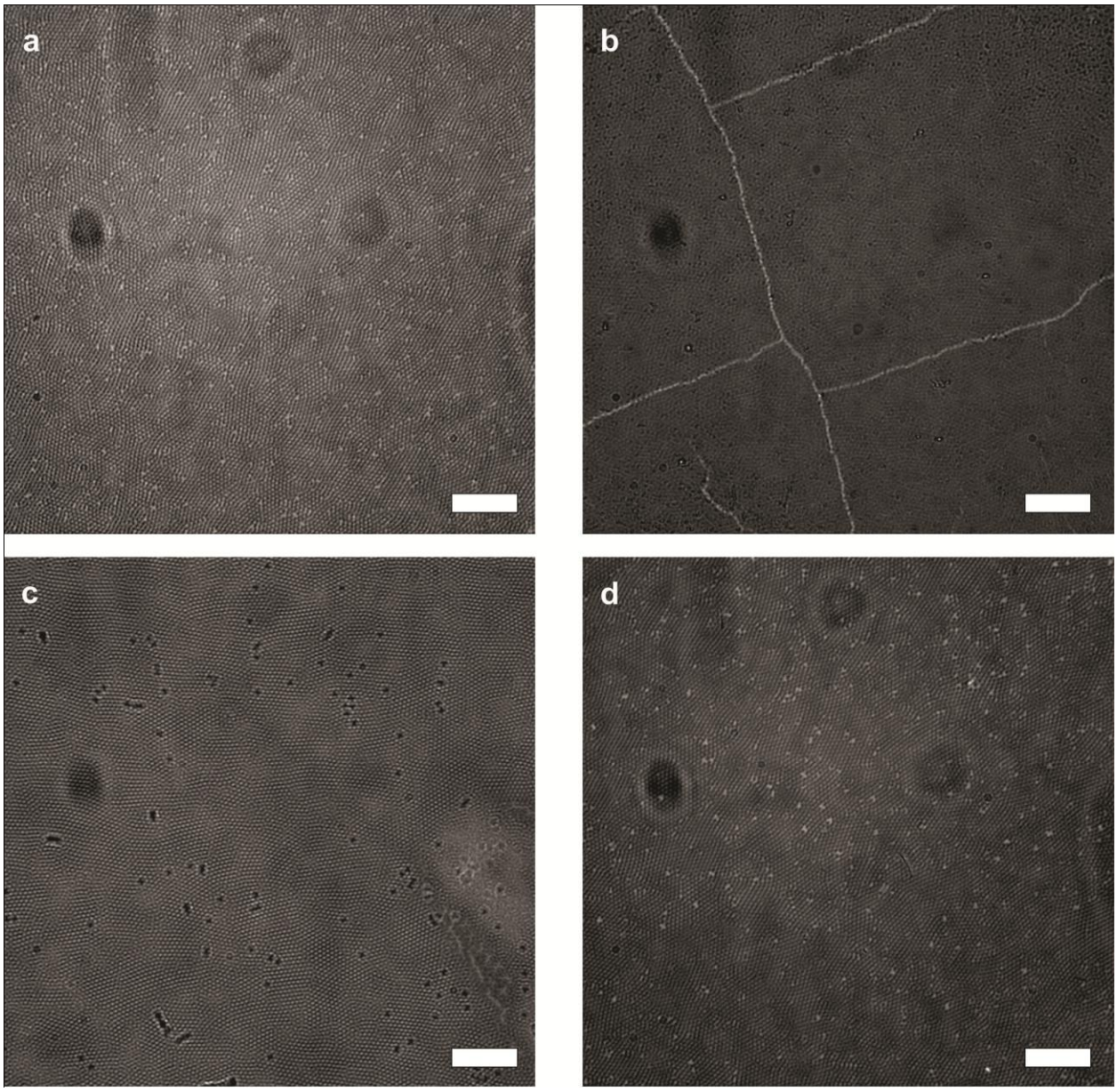

Figure 2-7. DIC microscopy images of an etalon fabricated using Ni for the bottom reflective layer and (a) Al, (b) Cu, (c) Ni, or (d) Ti for the top layers. In each image the scale bar is 10 μm.

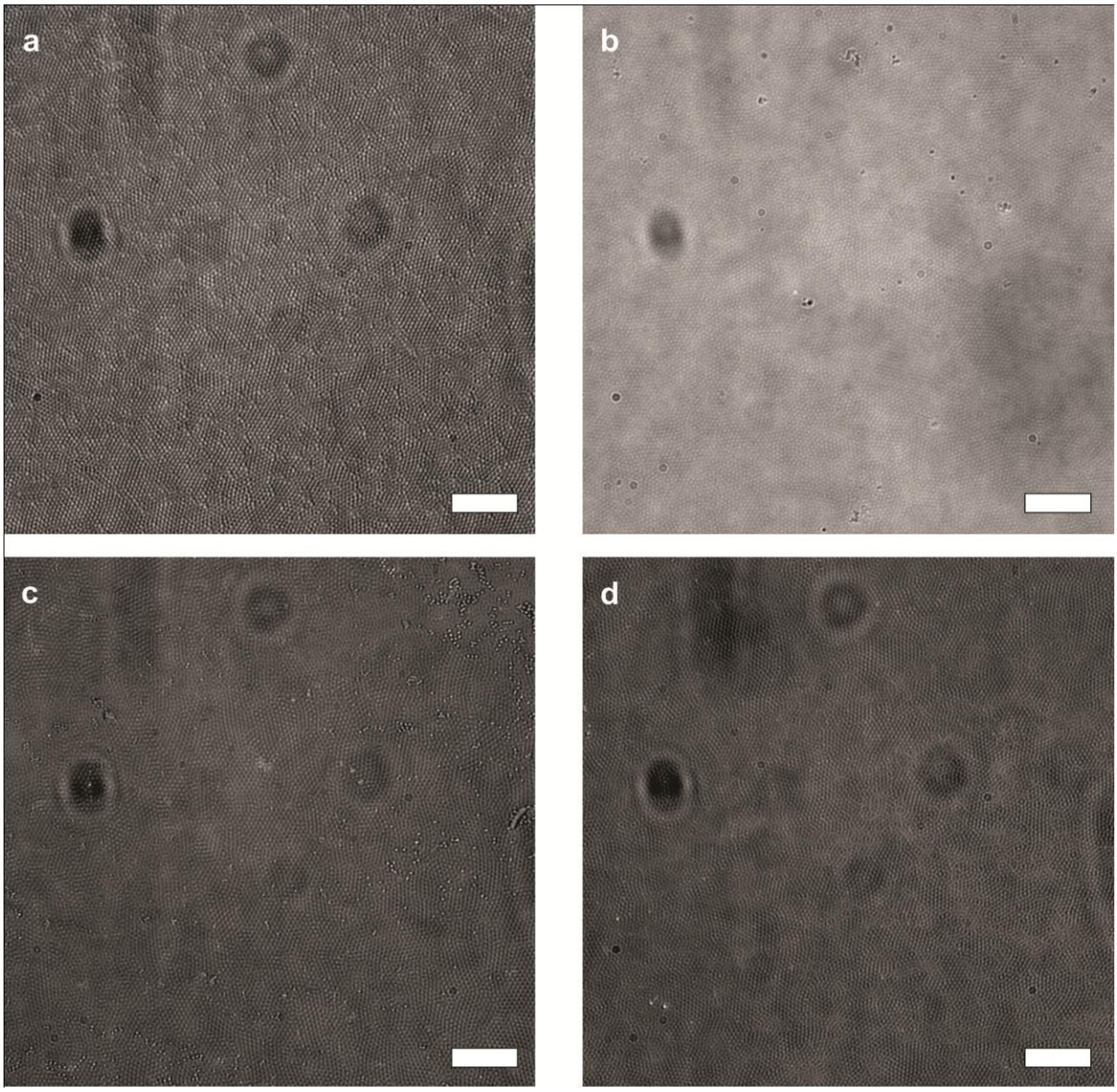

Figure 2-8. DIC microscopy images of an etalon fabricated using Ti for the bottom reflective layer and (a) Al, (b) Cu, (c) Ni, or (d) Ti for the top layers. In each image the scale bar is 10 μm.

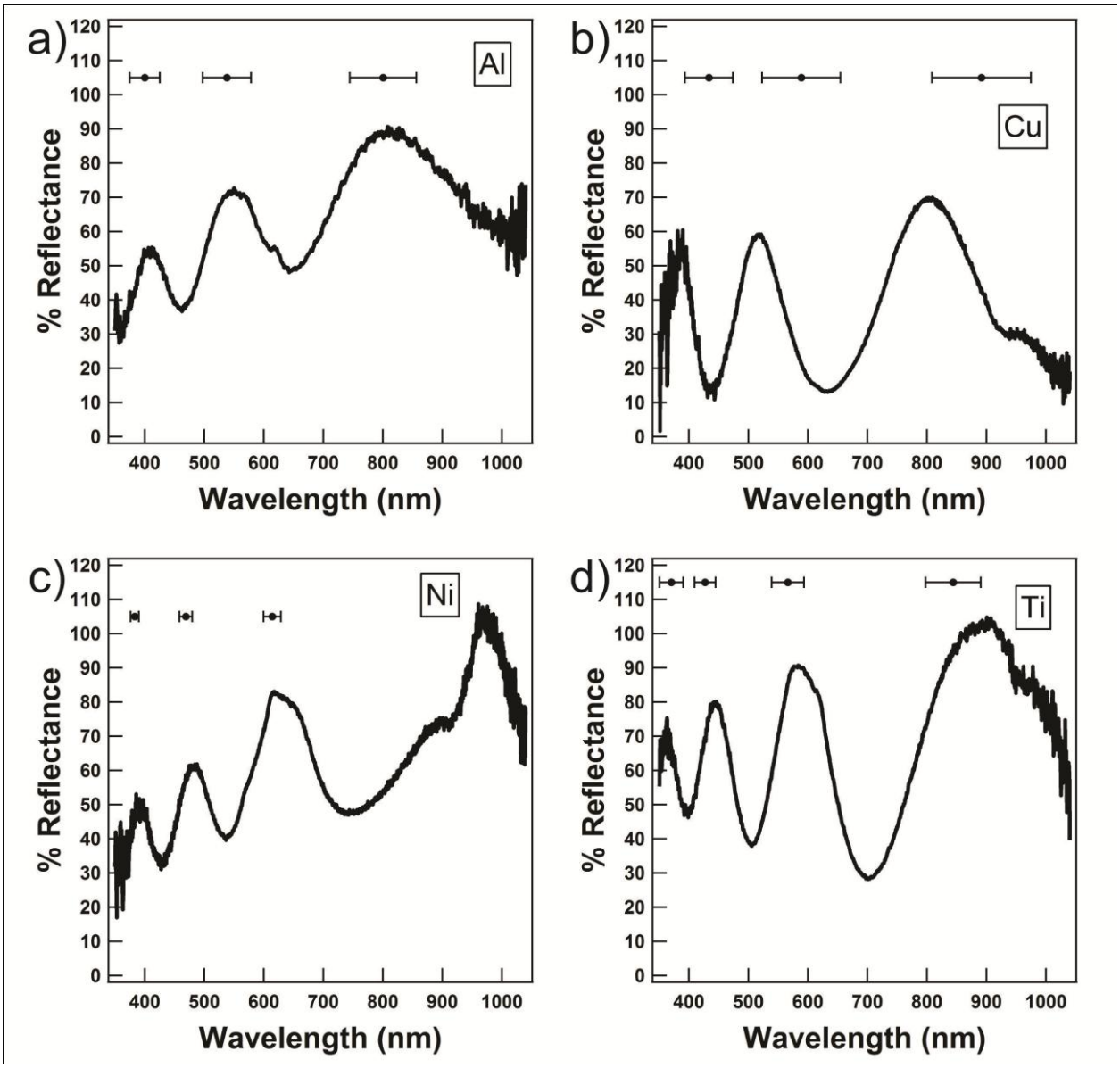

Figure 2-9. Reflectance spectra of an etalon fabricated using Al for the bottom reflective layer and (a) Al, (b) Cu, (c) Ni, or (d) Ti for the top layer. The marker above each peak depicts the average peak position for spectra collected on 3 random spots on the etalon, the error bars showing the standard deviation associated with the peak position.

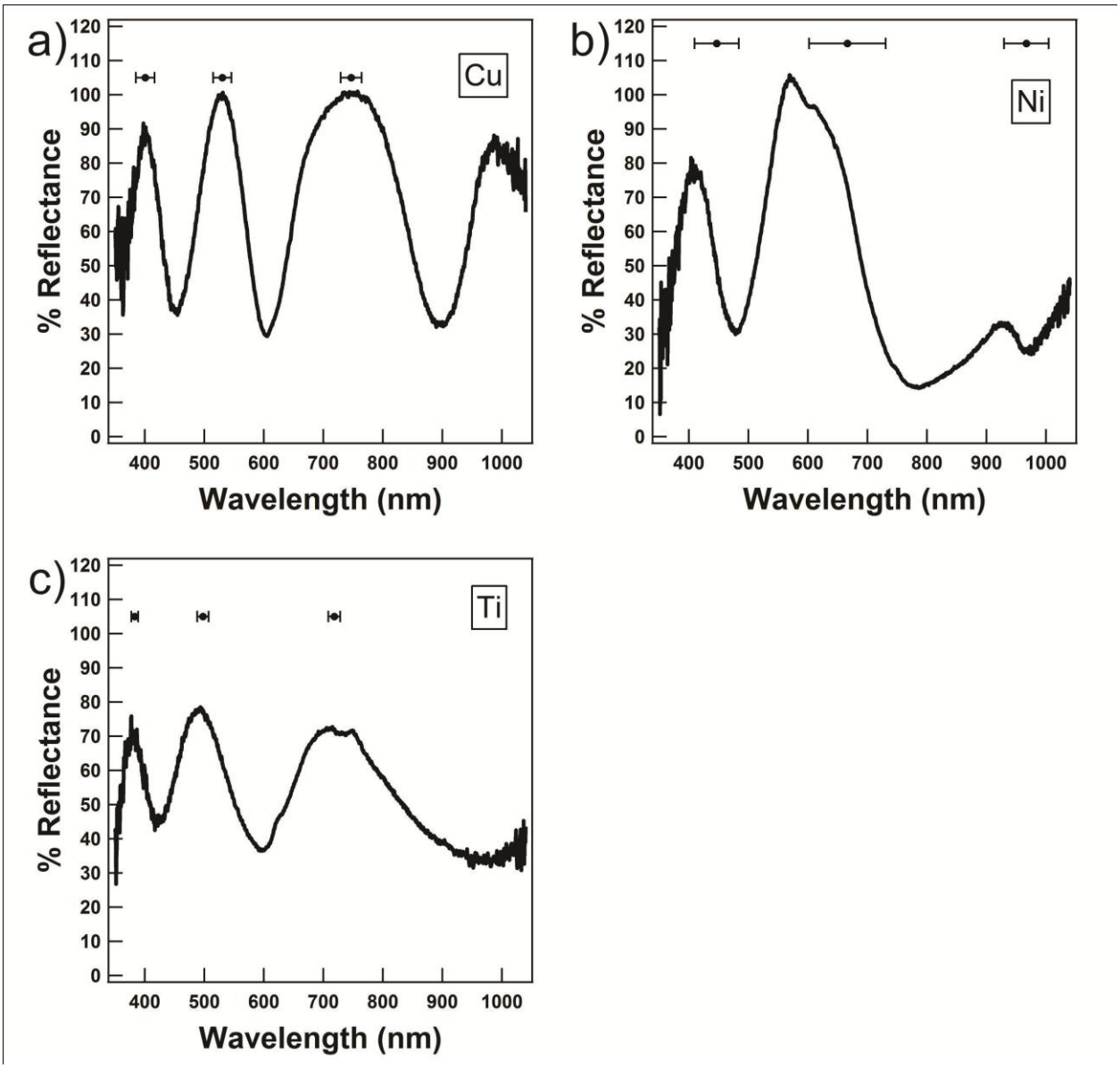

Figure 2-10. Reflectance spectra of an etalon fabricated using Cu for the bottom reflective layer and (a) Al, (b) Cu, or (c) Ni for the top layer. The marker above each peak depicts the average peak position for spectra collected on 3 random spots on the etalon, the error bars showing the standard deviation associated with the peak position.

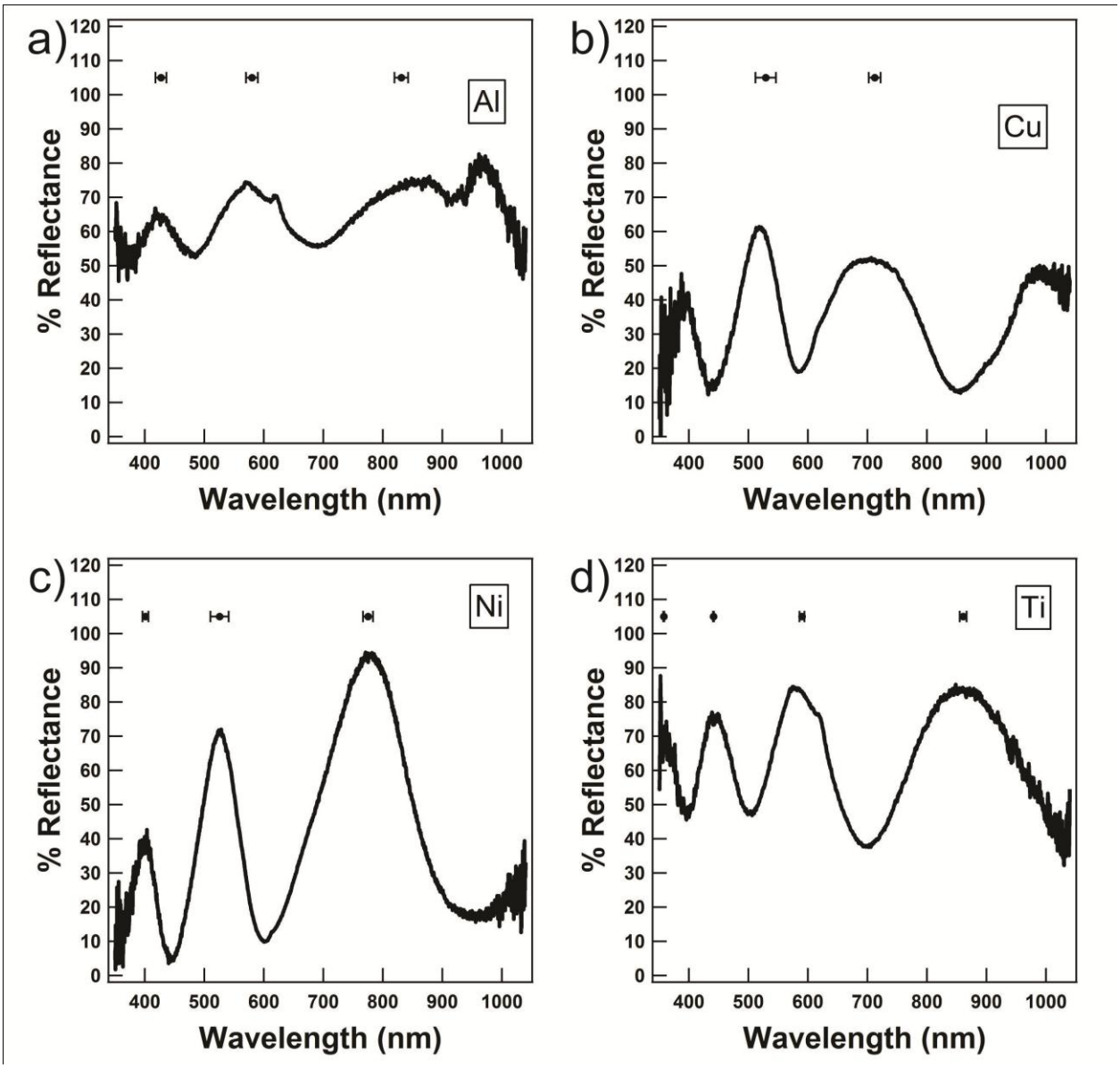

Figure 2-11. Reflectance spectra of an etalon fabricated using Ni for the bottom reflective layer and (a) Al, (b) Cu, (c) Ni, or (d) Ti for the top layer. The marker above each peak depicts the average peak position for spectra collected on 3 random spots on the etalon, the error bars showing the standard deviation associated with the peak position.

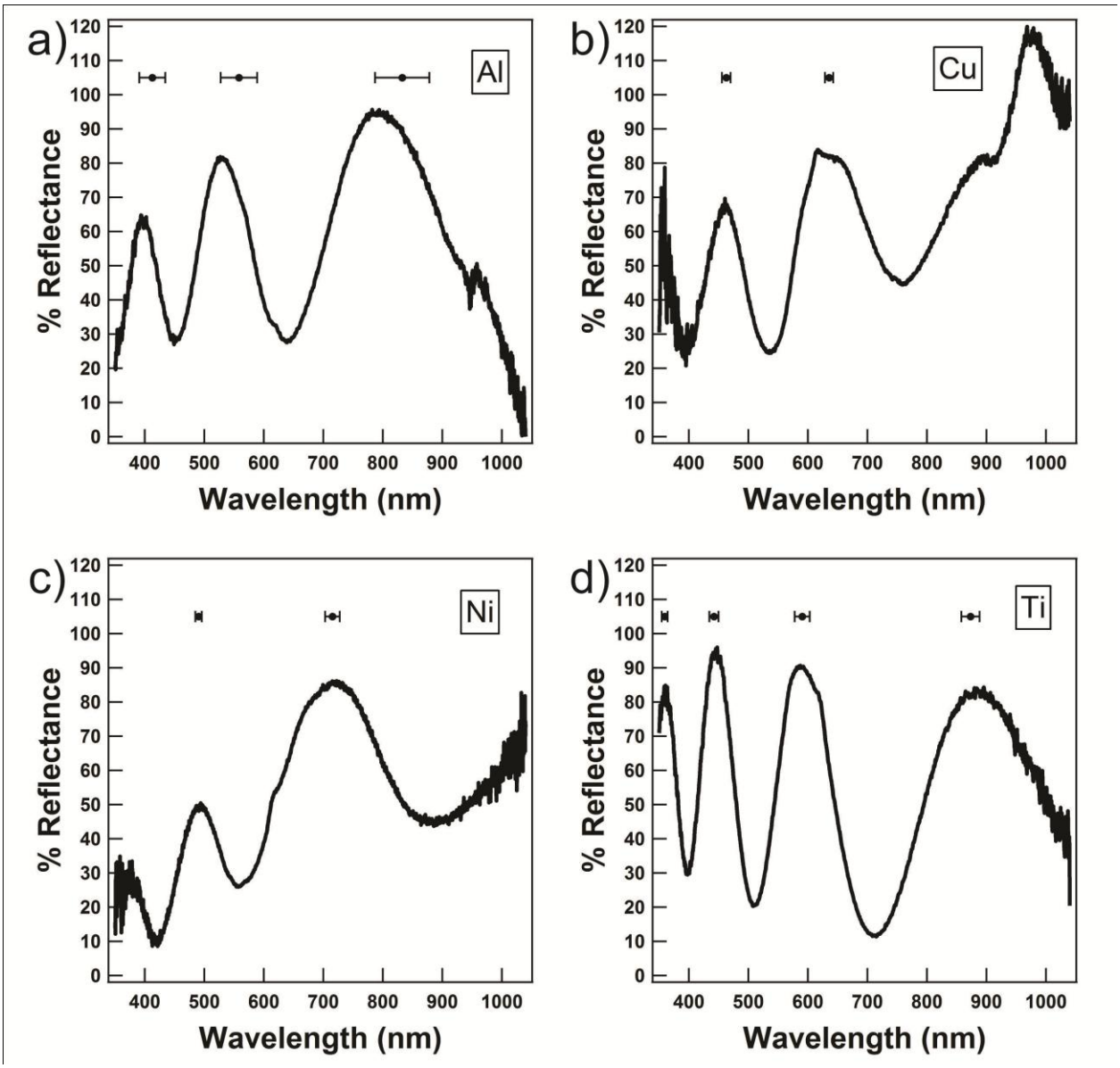

Figure 2-12. Reflectance spectra of an etalon fabricated using Ti for the bottom reflective layer and (a) Al, (b) Cu, (c) Ni, or (d) Ti for the top layer. The marker above each peak depicts the average peak position for spectra collected on 3 random spots on the etalon, the error bars showing the standard deviation associated with the peak position.

We note here that while etalons can be fabricated using different metals as the top and bottom layer, their stability over time is affected by the stabilities of the metals in a given solvent. Specifically, Al and Cu can degrade in DI water if left exposed for extended periods of time. In this case, tetrahydrofuran (THF) or methanol (MeOH) can be used in the place of water as part of the painting protocol. In this case though, more heterogeneous films were obtained, as is observed in Figure 2-5.

Finally, as has been shown in the past, when these assemblies are heated to above the VPT for the pNIPAm-based microgels, the devices change visual color and the peaks in the reflectance spectra shift toward lower wavelength.[42] While this is the case for the Au-based assemblies, it has yet to be shown that this is possible with the various metal combinations described. Figures 2-13 to 2-16 shows how λ_{max} for a single reflectance peak from various etalons varies as the solution temperature is increased from 25 °C to 40 °C. As can be seen, in each case the pNIPAm microgel-based etalons exhibited behavior similar to the Au-based etalons, indicating that the various metals do not affect the etalon's properties.

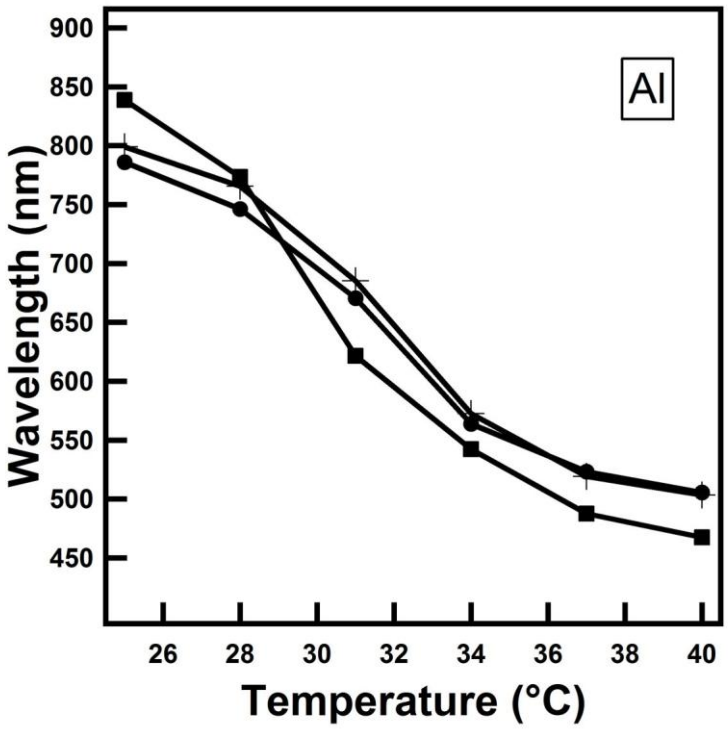

Figure 2-13. Plot of wavelength vs. temperature for a single peak in the reflectance spectrum of an etalon as the temperature is increased from 25 °C to 40 °C in 3 °C increments. Circles (●), triangles (▲), squares (■), and plus signs (+) correspond to etalons fabricated using Al for the bottom layer and Al, Cu, Ni, and Ti respectively for the top layer.

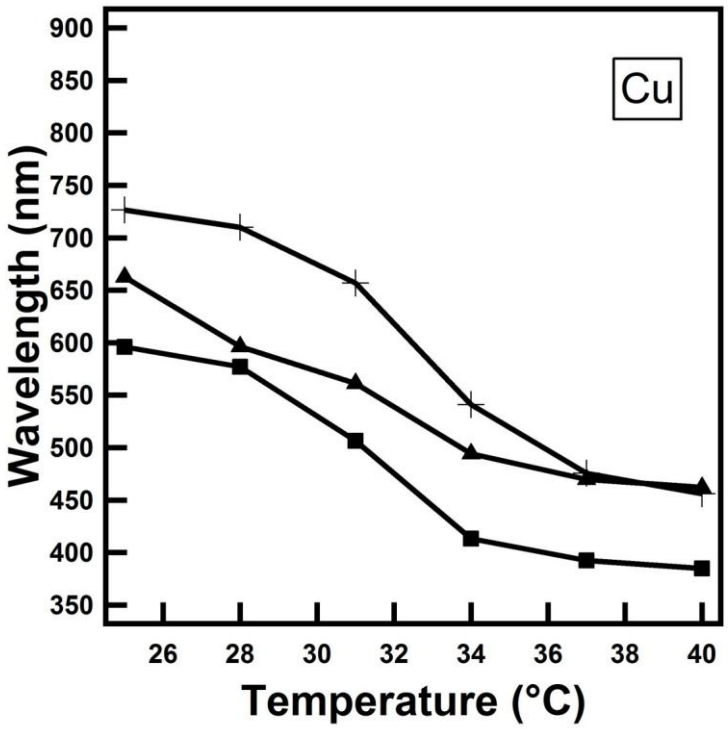

Figure 2-14. Plot of wavelength vs. temperature for a single peak in the reflectance spectrum of an etalon as the temperature is increased from 25 °C to 40 °C in 3 °C increments. Triangles (▲), squares (■), and plus signs (+) correspond to etalons fabricated using Cu for the bottom layer and Cu, Ni, and Ti respectively for the top layer.

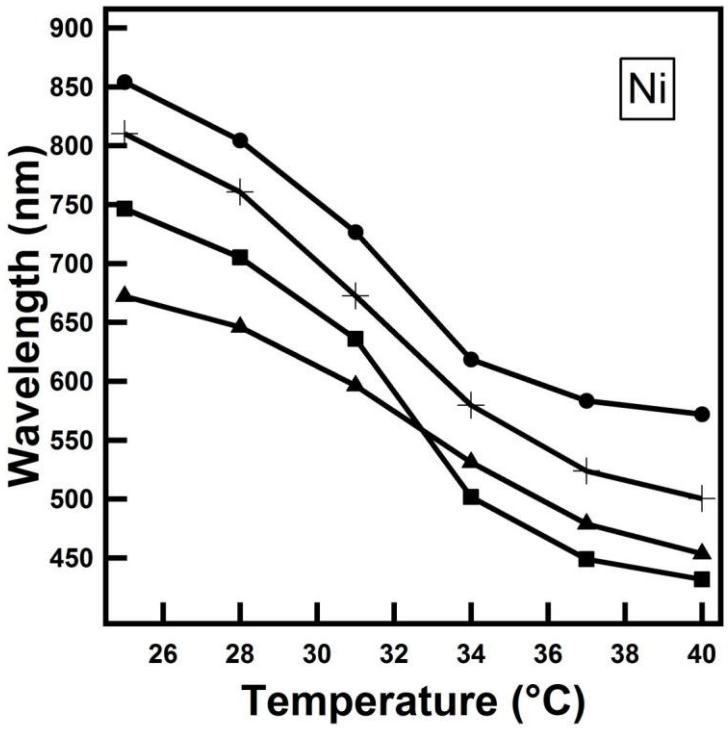

Figure 2-15. Plot of wavelength vs. temperature for a single peak in the reflectance spectrum of an etalon as the temperature is increased from 25 °C to 40 °C in 3 °C increments. Circles (●), triangles (▲), squares (■), and plus signs (+) correspond to etalons fabricated using Ni for the bottom layer and Al, Cu, Ni, and Ti respectively for the top layer.

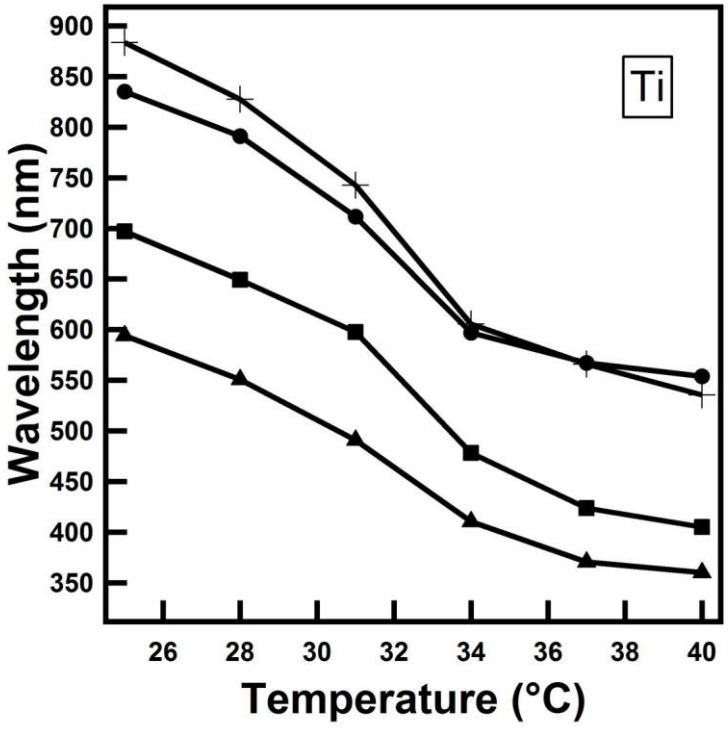

Figure 2-16. Plot of wavelength vs. temperature for a single peak in the reflectance spectrum of an etalon as the temperature is increased from 25 °C to 40 °C in 3 °C increments. Circles (●), triangles (▲), squares (■), and plus signs (+) correspond to etalons fabricated using Ti for the bottom layer and Al, Cu, Ni, and Ti respectively for the top layer.

2.4. Conclusions

A POC diagnostic device must not only be accurate, robust, and easy to use, but must also be amenable to large-scale fabrication. Therefore, to be viable, POC diagnostics must be comprised of inexpensive materials while retaining the accuracy and robustness of the device. Here we found that there was no distinguishable difference between etalons fabricated using Au, and more

affordable metals such as Al, Cu, Ni, and Ti. Microscopy images of the etalons were examined to develop a comparison between the alternate metal substrates and the standard Au based etalon. We determined that a monolithic jammed microgel layer was deposited on to the substrate regardless of which metal was used in the fabrication process. Reflectance spectroscopy was used to examine etalon optical properties and to determine if any the various metals affected the etalon's thermal responsivity. While reflectance peaks were seen at different wavelengths, each etalon fabricated exhibited a normal reflectance spectrum, and the peaks shift in response to temperature as expected.

Chapter 3

Effect of Confinement on the Transition Temperature of Poly (N-isopropylacrylamide)- Based Microgels

3.1. Introduction[2]

Poly (*N*-isopropylacrylamide) (pNIPAm) is one of the most well studied responsive polymers, known for its abrupt volume phase transition temperature (VPTT) at 32 °C in water.[12] That is, pNIPAm dissolved in water at room temperature exists as a fully solvated random coil, but becomes desolvated, and transitions to a dense globular state when the temperature of the water is > 32 °C. The transition is reversible if the water temperature is decreased to < 32 °C. The VPTT of uncrosslinked, linear pNIPAm in water, and the factors that affect it, has been extensively studied.[9, 11, 15, 39, 69, 73-79] Investigations of particular interest to the work here involve understanding how the addition of various solvents to the water pNIPAm was dissolved in influenced the VPTT.[8, 10, 40, 41, 69, 80-86] In one study, Tirrell and coworkers showed that the VPTT of linear pNIPAm depends on the volume fraction of methanol (MeOH) (and other solvents) mixed in the water pNIPAm was dissolved in. Specifically, when the volume fraction of MeOH in water was increased, the VPTT of pNIPAm decreased. A minimum in the VPTT was achieved when the solution reached ~ 55% (v/v) MeOH. As the solution concentration of MeOH was further increased, the VPTT increases rapidly until ~ 65% (v/v) MeOH is reached after which no transition was observed in the

[2] *A version of this chapter has been submitted for publication.*

measurable temperature range. The variation of the VPTT as a function of MeOH concentration is an effect of cononsolvency; cononsolvency is a phenomenon that arises when a polymer is soluble in two pure solvents but becomes insoluble in mixtures of the two. While much is known about the behavior of linear pNIPAm (specifically cononsolvency),[8, 40, 41, 82, 85, 86] relatively little is known about how the various factors affect the VPTT of pNIPAm-based microgels.[10, 69, 83] Richtering and coworkers recently showed that the general behavior of pNIPAm-based microgels in MeOH:water mixtures was similar to linear pNIPAm.[10] That is, the VPTT for pNIPAm-based microgels decreases to a minimum of ~ -10 °C at ~ 55% methanol (v/v) in water.

Previously, we have shown that devices constructed by sandwiching a pNIPAm-based microgel layer between two semi-transparent Au layers exhibit unique optical properties.[42, 43, 49, 55] Figure 3-1 shows a schematic of the device, which are referred to as pNIPAm microgel-based etalons. They exhibit unique optical properties due to their structure, which allows light to enter and resonate in the microgel-based cavity. The light resonating in the cavity can undergo constructive/destructive interference, which yields visual color and characteristic multipeak spectra.[45] Figure 3-2 shows a representative spectrum from a typical pNIPAm microgel-based etalon used in this study. This position of the peaks in these spectra can be predicted from equation (1):

$$\lambda m = 2nd \cos\theta \quad (1)$$

where n is the refractive index of the dielectric material, d is the distance between the reflective surfaces, m is the peak order, and θ is the angle of incident light. From the equation it is clear that the wavelength of reflected light (λ) directly depends on both the refractive index of the dielectric, and the thickness of the dielectric layer.

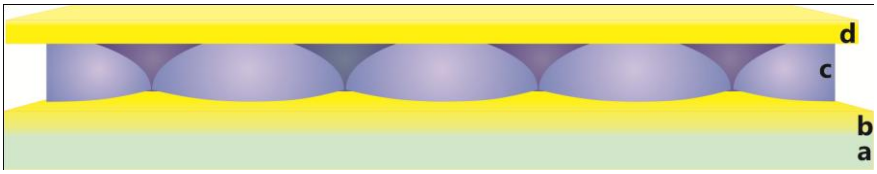

Figure 3-1. Schematic depiction of an etalon where (a) is the glass substrate base (b) and (d) are the Au reflective surfaces and (c) is the pNIPAm microgel-based layer.

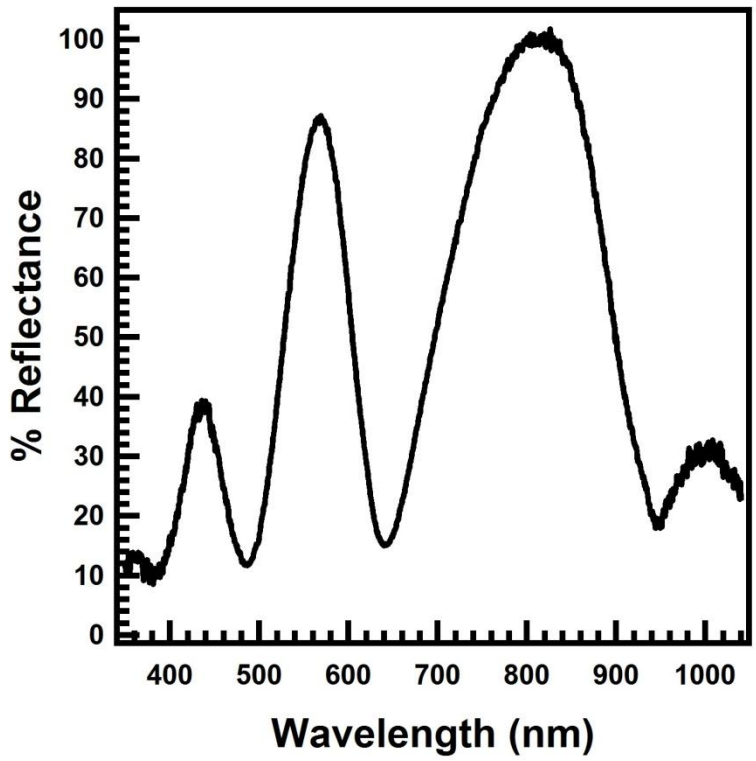

Figure 3-2. Characteristic reflectance spectrum of a pNIPAm microgel-based etalon.

Interestingly, these devices exhibit optical properties that depend on the temperature of the water they are immersed in. Specifically, we have shown that λ depends on temperature, shifting to lower wavelengths (blue shifting) as the temperature of the water is increased above the VPTT of the pNIPAm-based microgels. This change of λ with temperature is a direct result of the microgels decreasing in diameter as the solution temperature approaches, and exceeds, pNIPAm's VPTT causing the etalon's Au layers to approach one another. This can be predicted from equation (1). The data shows that the VPTT for the microgels in the etalon is close to the VPTT of microgels dispersed in water.

In this experiment, we examine the VPTT of pNIPAm-based microgels, both dispersed in solution and immobilized between the two Au layers of the etalon, in aqueous solutions of various MeOH (v/v) concentrations. The results of this study have shown that the VPTT for microgels in an etalon is close to the VPTT of microgels dispersed in water. This allowed us to further investigate the cononsolvency behavior of the pNIPAm-based microgels, which revealed a VPTT for the pNIPAm-based microgels at MeOH concentrations much higher than has been previously observed in other studies. As this is the case, we feel that the etalon offers an effective means to investigate the fundamental properties of pNIPAm-based microgels further.

3.2. Materials and Methods

Materials: *N*-Isopropylacrylamide (NIPAm) was purchased from TCI (Portland, Oregon) and purified by recrystallization from hexanes before use (ACS reagent grade, EMD, Gibbstown, NJ). *N,N'*-methylenebisacrylamide (BIS, 99%) and ammonium persulfate (APS, 98% +) were obtained from Sigma-Aldrich (Oakville, Ontario) and were used as received. Methanol (MeOH, 99.8%) was purchased from Caledon Chemicals (Georgetown, Ontario) and was used as received. All deionized (DI) water was filtered through a Milli-Q Plus System (Millipore, Billerica, MA) to a resistivity of 18.2 MΩ·cm. Cr/Au annealing was done in a Thermolyne muffle furnace from Thermo Fisher Scientific (Ottawa, Ontario). Anhydrous ethanol was obtained from Commercial Alcohols (Brampton, Ontario). Fisher's Finest glass cover slips, 25 x 25 mm, were purchased from Fisher Scientific (Ottawa, Ontario). Cr flakes (99.999%) were

purchased from ESPI (Ashland, Oregon). Au shot (99.99%) was purchased from MRCS Canada (Edmonton, Alberta).

Microgel Synthesis: PNIPAm-based microgels were synthesized via surfactant free, free radical precipitation polymerization as previously described.[87] The total monomer concentration was 140 mM, and was 95% N-isopropylacrylamide (NIPAm) and 5% N,N'-methylenebisacrylamide (BIS, crosslinker). The monomer, NIPAm (13.3 mmol) and crosslinker, BIS (0.7 mmol) were dissolved in 80 mL of deionized water in a 150 mL beaker while being stirred. The mixture was then filtered, through a 0.2 μm filter on a 20 mL syringe, into a 250 mL round bottom flask. The beaker was then rinsed with an additional 19 mL of deionized water, which was also filtered into the round bottom flask. The round bottom flask was then fitted with a temperature probe, a condenser, and a N_2 needle inlet. The reaction mixture was heated to 65 °C at a rate of 30 °C per hour, while being purged with N_2 and stirred at a rate of 450 rpm. Once a constant temperature was reached (~90 minutes) the N_2 needle was removed from the solution, while keeping a N_2 atmosphere, and APS (0.2 mmol) dissolved in 1 mL of deionized water was added to the reaction mixture to initiate the reaction. The reaction was then allowed to proceed for 4 hours, then removed from heat and allowed to cool to room temperature overnight. Aggregates were then removed by filtering the polymer mixture through Whatman #1 qualitative filter paper from Fisher Scientific (Ottawa, Ontario), and rinsing with deionized water. The solution was then transferred to centrifuge tubes and centrifuged at ~8400 relative centrifugal force (RCF) at 22 °C for 30 minutes until the microgels formed a

concentrated pellet at the bottom of the tubes. The supernatant was then removed and the microgels were resuspended in 12 mL of deionized water. This was done a total of 6 times to remove left over monomer and linear polymer from the microgels.

Etalon fabrication: The Cr/Au layers were deposited using a Torr International Inc. model THEUPG thermal evaporation system (New Windsor, NY). For each sample a 25 x 25 mm glass substrate was rinsed copiously with ethanol and dried under N_2 before metal deposition under vacuum (low 10^{-6} torr range). The Au substrates were annealed in a Thermo Scientific thermolyne muffle furnace from Fisher (Waltham, MA) at 250 °C for 3 hours before use. Microgels were then applied directly to the metal layer using the previously described painting protocol.[42] Briefly, microgel solutions were centrifuged at ~8400 relative centrifugal force (RCF) for 60 minutes at 22 °C to form a concentrated microgel pellet in the centrifuge tube. The metal substrates were then rinsed with ethanol and dried under N_2 before being placed on a hot plate at 35 °C. Once on the hot plate, 40 µL of the concentrated microgels was pipetted on to the substrate and spread evenly using the side of the micropipette tip. The substrate was then rotated and the microgels were spread more as they began to dry. Once evenly covered the microgels were allowed to dry for 2 hours and then rinsed copiously with DI water until all excess microgels (microgels not directly adhered to the metal layer) were removed. The substrates were subsequently soaked overnight in deionized water. After soaking overnight, the substrates were

rinsed once more with DI water and dried with N_2 gas, then coated with a second metal layer using the described method.

Reflectance Spectroscopy: Reflectance was measured using a USB2000+ spectrophotometer, an HL-2000-FHSA halogen light source, and a R400-7-VIS-NIR optical fiber reflectance probe from Ocean Optics (Dunedin, Florida). All data was recorded using Spectra Suite software from Ocean Optics. The reflectance was measured in the range of 350 to 1039 nm and was done in a custom made chamber for sample positioning and temperature control. Experiments began at a temperature well below the transition temperature and the temperature of the solvent was increased in 3 °C increments, the spectra being saved after each increment. To reach low temperatures, the chamber was cooled using dry ice, and regulated by the temperature controller. The experimental apparatus used can be seen in figure 2-2.

Light Scattering Studies: Transmission of light through microgel solutions was measured using a USB2000+ spectrophotometer, an HL-2000-FHSA halogen light source, and UV/VIS optical fiber from Ocean Optics (Dunedin, Florida). All data was recorded using Spectra Suite software from Ocean Optics. The transmission of light was measured through a 10 mm quartz spectrophotometer cell from Starna Cells Inc. (Atascadero, CA). All measurements were done in a custom-made cuvette holder with precise temperature control. Experiments began at a temperature well below the transition temperature and the temperature of the solution in the cuvette was increased in 3 °C increments, the spectra being saved after each increment. To reach low

temperatures, the chamber was cooled using dry ice, and regulated by the temperature controller. This experimental apparatus can be seen in figure 3-3.

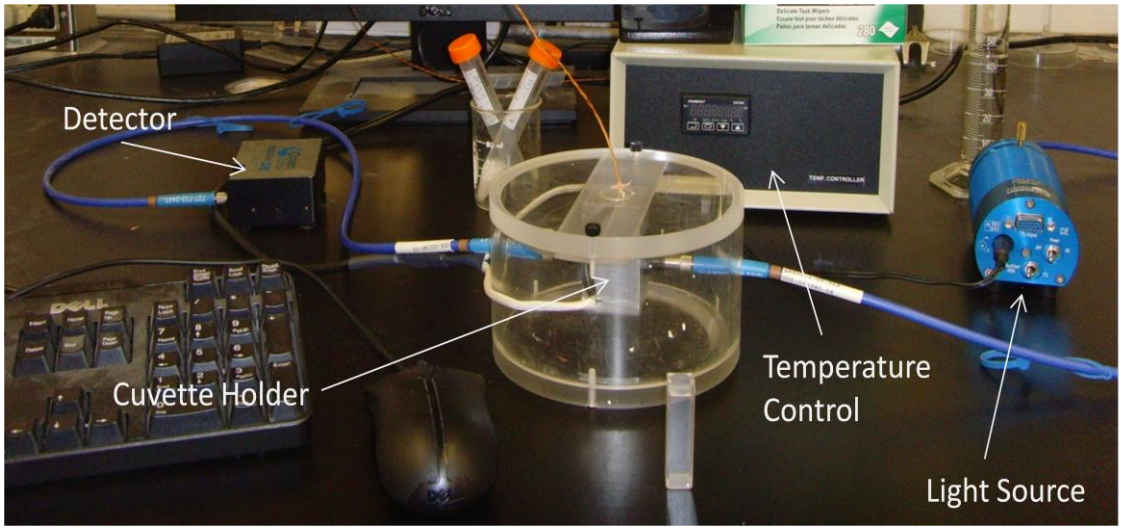

Figure 3-3. Light scattering set up used in experiments.

3.3. Results and Discussion

For many applications of pNIPAm microgel-based etalons, it is important to obtain a complete understanding of how their confinement between the etalon's two Au mirrors affects their behavior. To investigate this, we determined the VPTT for pNIPAm-based microgels in etalons. Once the VPTT for the microgels in the etalons was determined, we compared it to the VPTT for the microgels in solution. To accomplish this, the microgels or etalon were/was dissolved or immersed in water. The transmitted light intensity (microgels in solution), and light reflection (microgels in etalons) was measured as the solution temperature

was increased from a value well below the microgel's transition temperature to a value above the transition temperature in 3 °C increments. In both cases, a special apparatus was custom built to allow for temperature control and sample stability. For the microgels in solution, the intensity of light transmitted through the cuvette at 500.12 nm was monitored as a function of temperature. For the etalons, reflectance spectra were obtained at the various temperatures, and the position of the m = 2 and 3 peak was plotted as a function of temperature.

Plotted in Figure 3-4 is the variation of the transmitted light intensity at 500.12 nm for the microgels in solution and the percent reflectance from a single reflectance peak obtained from the etalon. In both cases, the VPTT was determined by drawing a tangent to the curve before and after the VPTT, and a tangent to the curve at the inflection point. As can be seen in Figure 3-5, this leads to two intersection points, on the low and high temperature side of the curve. The midpoint of those two intersection points was the VPTT. In this case, the VPTT for the microgels in solution and in the etalon was similar; 29.9 °C for the microgels is solution and 29.6 °C for the microgels in the etalon.

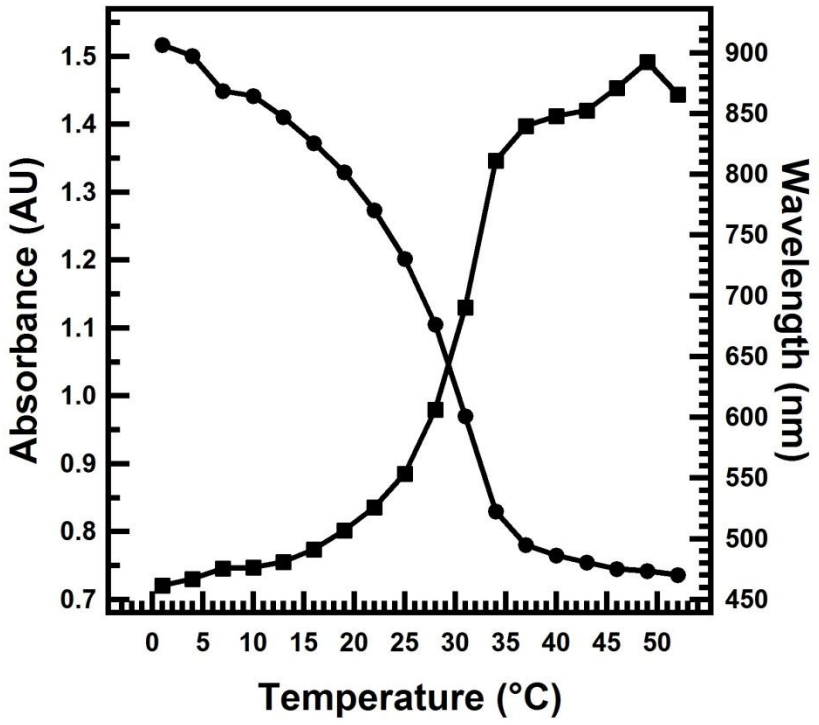

Figure 3-4. (left axis, ■) The variation of the "absorbance" or transmission of light of 500.12 nm through a solution of microgels as a function of temperature. (right axis, ●) The variation of λ for a microgel-based etalon as a function of temperature. Solution was DI water in both cases.

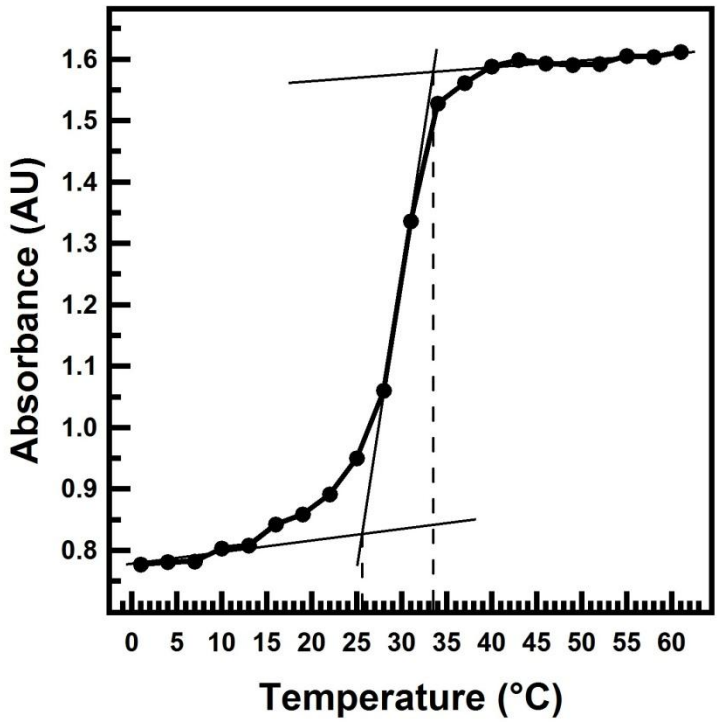

Figure 3-5. Example of how VPTT was calculated. Tangent lines were drawn to the curve before and after the transition, and to the steepest part of the curve in the transition region. Lines were extrapolated to the x-axis where the tangent lines intersect. The midpoint of those two x values was taken as the VPTT.

Since confinement has no noticeable influence on the VPTT of the pNIPAm-based microgels, we reasoned that the etalon structure should be useful for studying some fundamental properties of pNIPAm-based microgels that are not possible (or extremely difficult) to study using any other technique. We chose to investigate cononsolvency of pNIPAm-based microgels. As is well known for linear pNIPAm, the VPTT depends on the "pure" solvent it is dissolved in, and

oftentimes varies upon the addition of one solvent to the solvent the pNIPAm is dissolved in. Sometimes this is a result of cononsolvency.[8, 40, 41, 82, 85, 86]

We initially determined the VPTT for the microgels in solution in the same manner as indicated above for the microgels in water. This was for comparison to the data obtained for the pNIPAm microgel-based etalons. That is, for each solution of the various MeOH concentrations in water, the transmitted light intensity was monitored at 500.12 nm as a function of temperature and the approach in Figure 3-5 was used to extract the VPTT. A complete set of data can be seen in Figures 3-6 to 3-14, while the VPTTs for the various solutions can be seen in Figure 3-23. We point out here that it was not always straightforward to define the tangents, and were occasionally approximated; stars in the Figure indicate those particular points. By looking at the data, it is apparent that the trend follows what was observed by Tirrell and coworkers for linear pNIPAm in solution, although the absolute values of the VPTT is much lower in the case of the microgels. Furthermore, the MeOH concentration where the minimum VPTT is reached is considerably different than previously observed. From the data we can see that the VPTT for the microgels in solution decreases until 65% methanol is reached, after which point the VPTT increases appears to increase with increasing MeOH concentration, although the VPTT at the high MeOH concentrations is very difficult to determine. Again, the data points that have a high degree of uncertainty are indicated with stars in Figure 3-23.

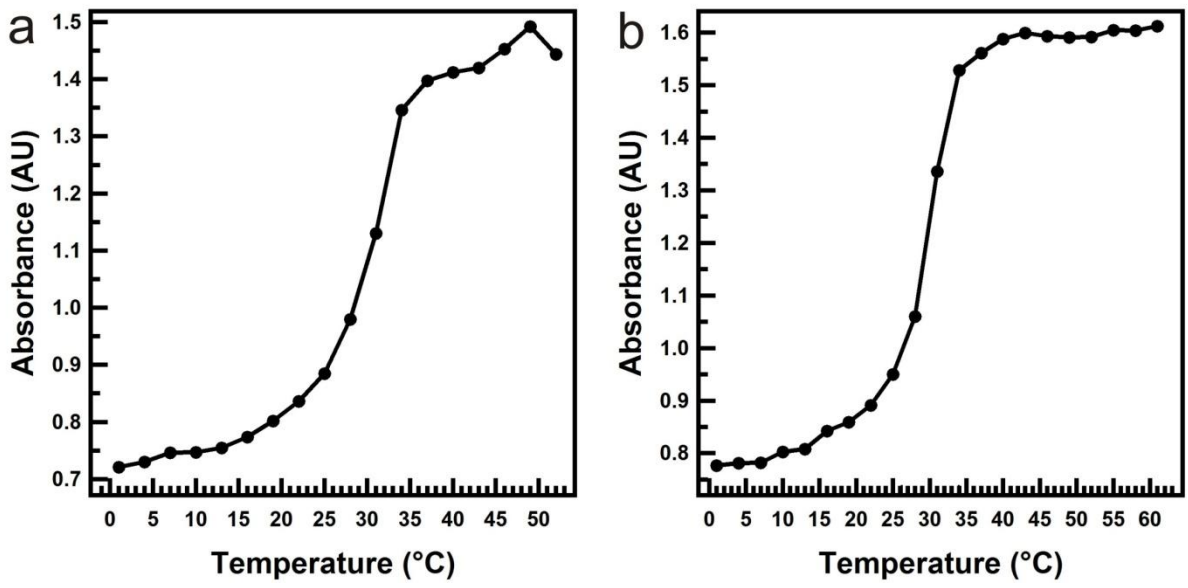

Figure 3-6. Plot of absorbance vs. temperature for two pNIPAm microgel solutions a and b as the temperature is increased in increments of 3 °C. The solvating solution is 0% methanol by volume.

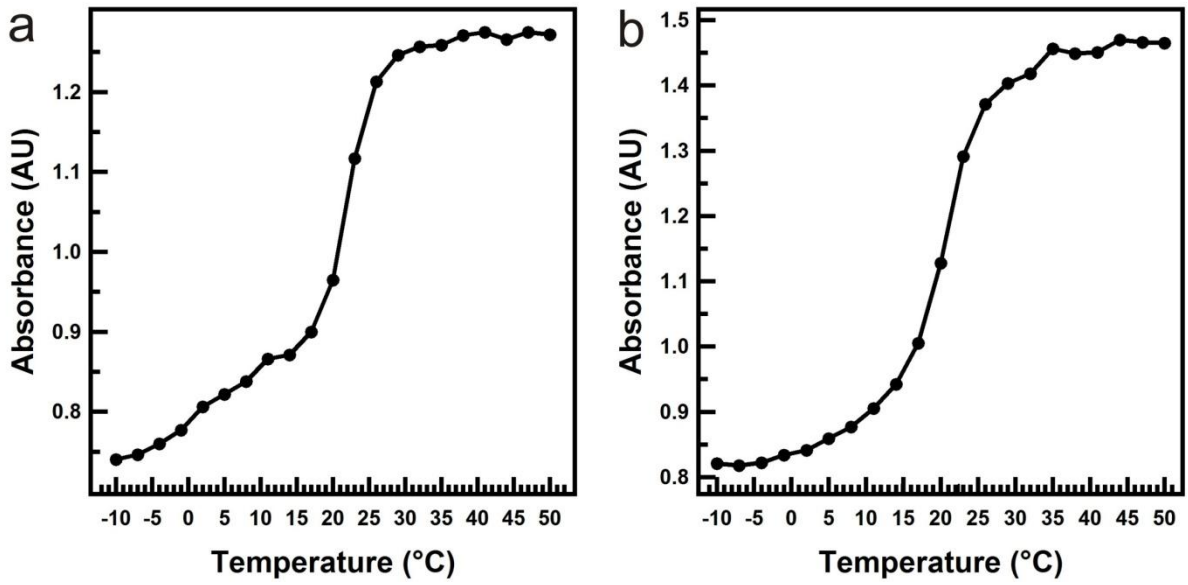

Figure 3-7. Plot of absorbance vs. temperature for two pNIPAm microgel solutions a and b as the temperature is increased in increments of 3 °C. The solvating solution is 20% methanol by volume.

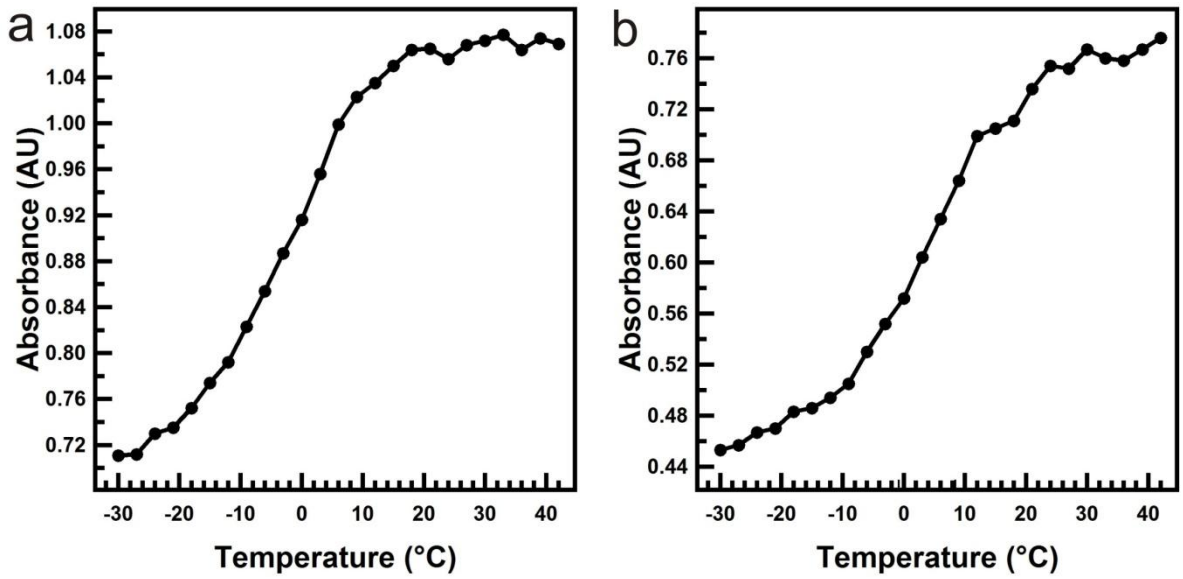

Figure 3-8. Plot of absorbance vs. temperature for two pNIPAm microgel solutions a and b as the temperature is increased in increments of 3 °C. The solvating solution is 40% methanol by volume.

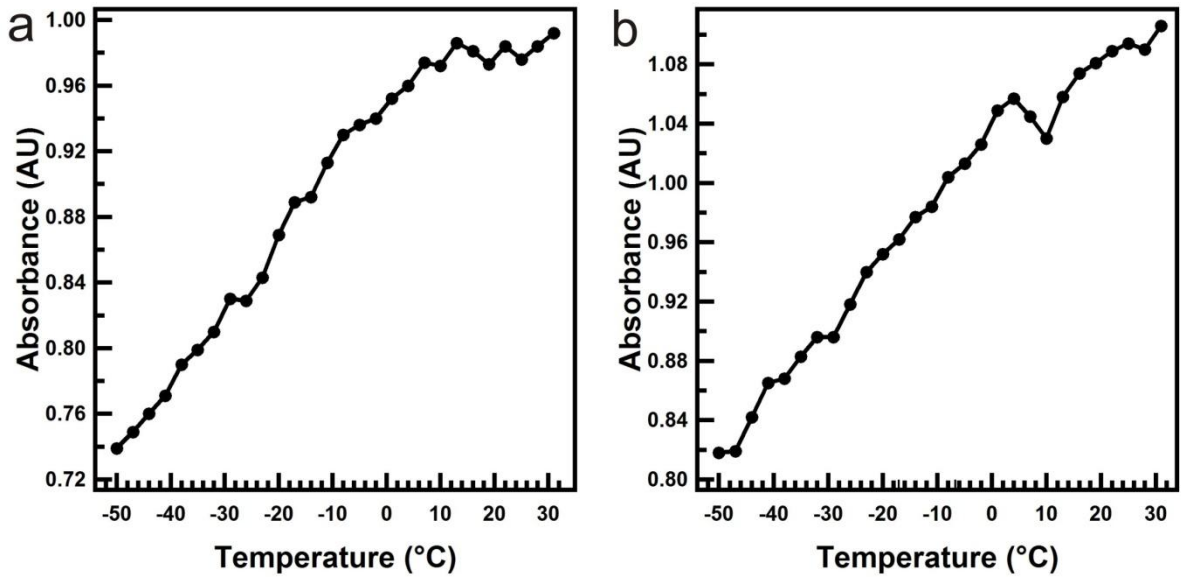

Figure 3-9. Plot of absorbance vs. temperature for two pNIPAm microgel solutions a and b as the temperature is increased in increments of 3 °C. The solvating solution is 55% methanol by volume.

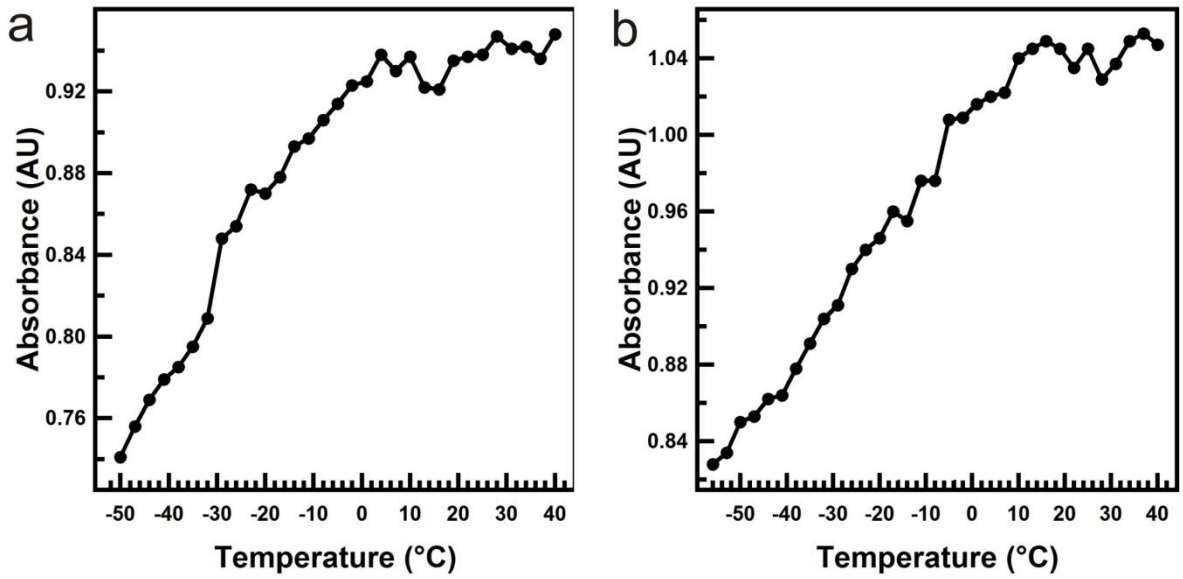

Figure 3-10. Plot of absorbance vs. temperature for two pNIPAm microgel solutions a and b as the temperature is increased in increments of 3 °C. The solvating solution is 60% methanol by volume.

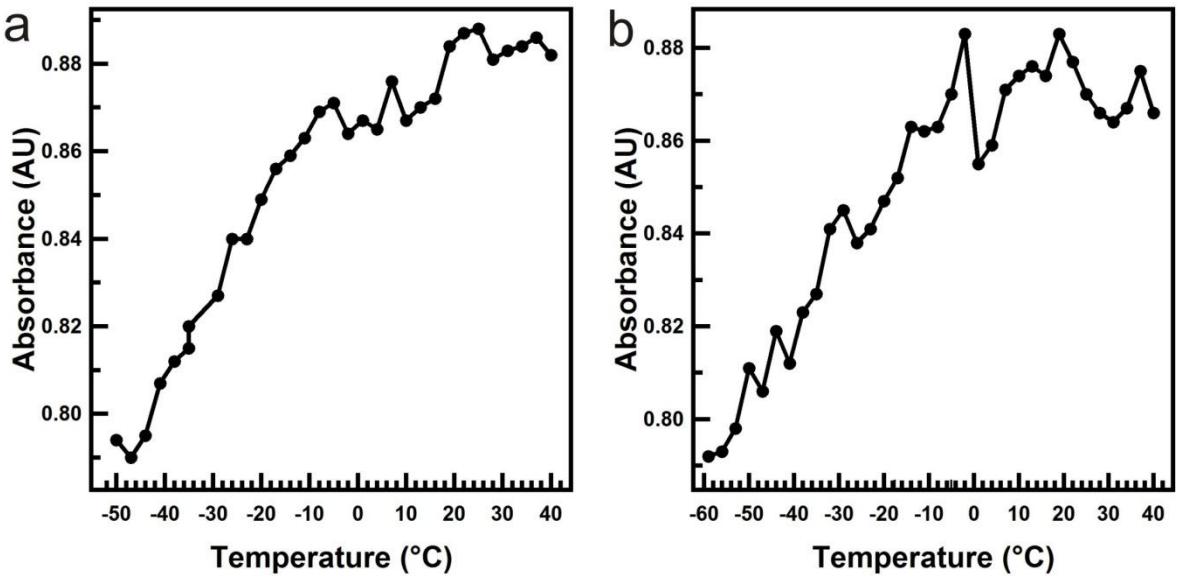

Figure 3-11. Plot of absorbance vs. temperature for two pNIPAm microgel solutions a and b as the temperature is increased in increments of 3 °C. The solvating solution is 65% methanol by volume.

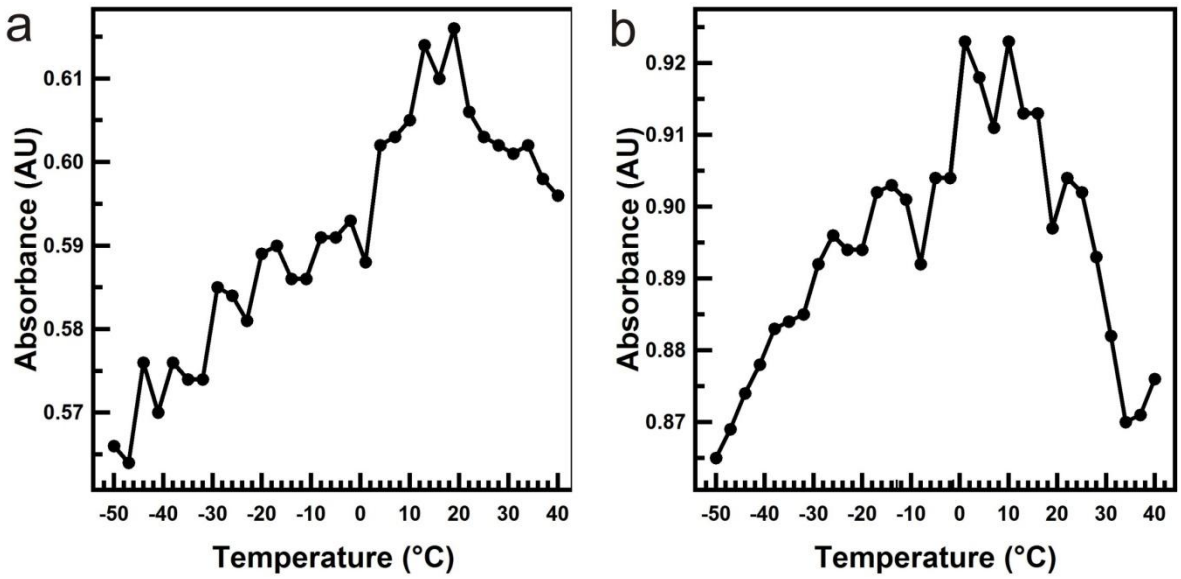

Figure 3-12. Plot of absorbance vs. temperature for two pNIPAm microgel solutions a and b as the temperature is increased in increments of 3 °C. The solvating solution is 70% methanol by volume.

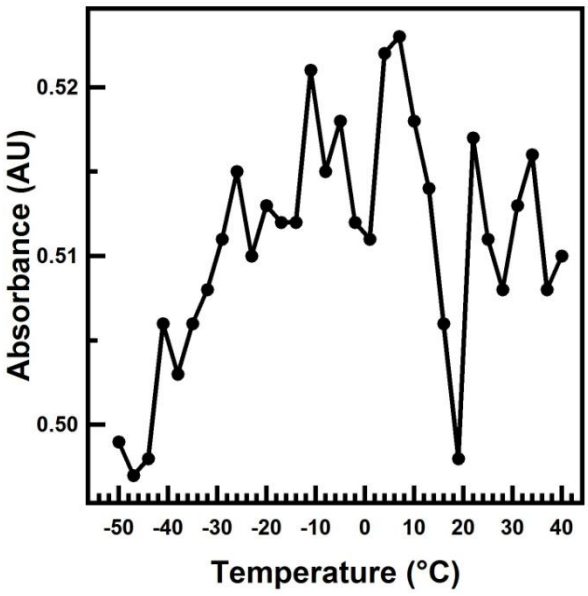

Figure 3-13. Plot of absorbance vs. temperature for pNIPAm microgel solution as the temperature is increased in increments of 3 °C. The solvating solution is 75% methanol by volume.

For comparison, pNIPAm microgel-based etalons were fabricated and the VPTT for the microgels was determined in the same manner as above. A complete set of data at the various MeOH concentrations in water can be seen in Figures 3-14 to 3-22, while the VPTTs for the various solutions can be seen in Figure 3-23. Again, we observe similar behavior for the microgels in etalons compared to the microgels in solution. Specifically, the VPTT decreases dramatically as the concentration of MeOH in water increases. In this case though, a significant transition magnitude is observed at each MeOH concentration, see Figure 3-24, even though the tangents may be difficult to define. What is most interesting about these data is that it does not follow the

same trends as observed by Tirrell for linear pNIPAm and by Richtering for pNIPAm-based microgels in solution. In fact, it is widely accepted that there is no VPTT for pNIPAm above ~65% MeOH in water, while our data indicates that there is a VPTT, at very low temperature. In fact, there is even an observable VPTT up to 80% methanol. Again, we feel that this is a result of the pNIPAm microgel-based etalons allowing us to observe the VPTT, as compared to other techniques where the VPTT may not be observed.

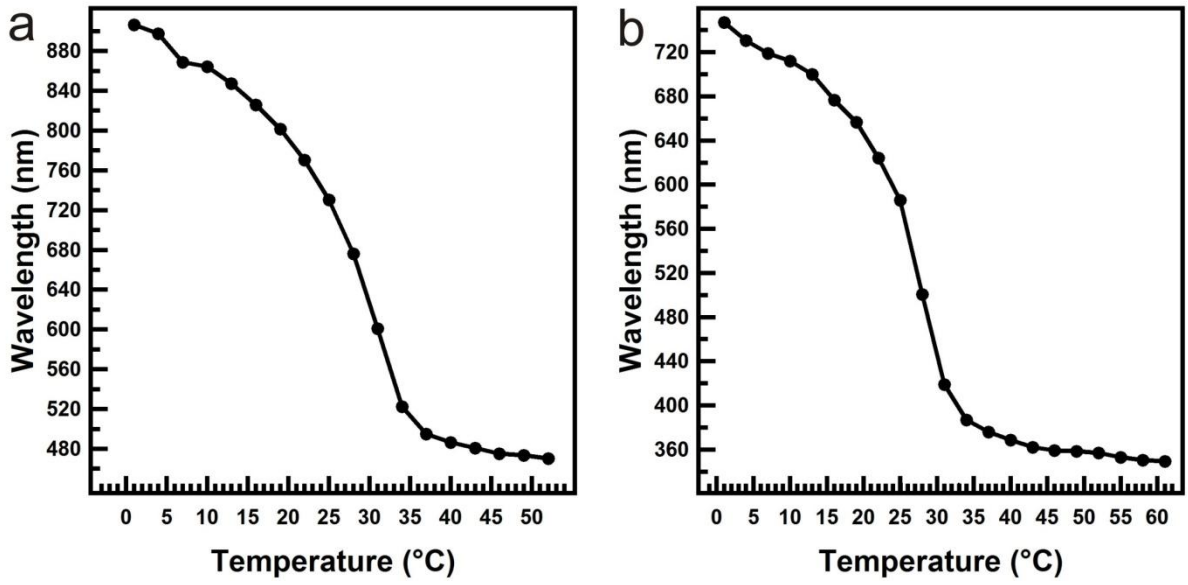

Figure 3-14. Plot of wavelength vs. temperature for a single peak in the reflectance spectrum of two etalons a and b as the temperature is increased in increments of 3 °C. The solvating solution is 0% methanol by volume.

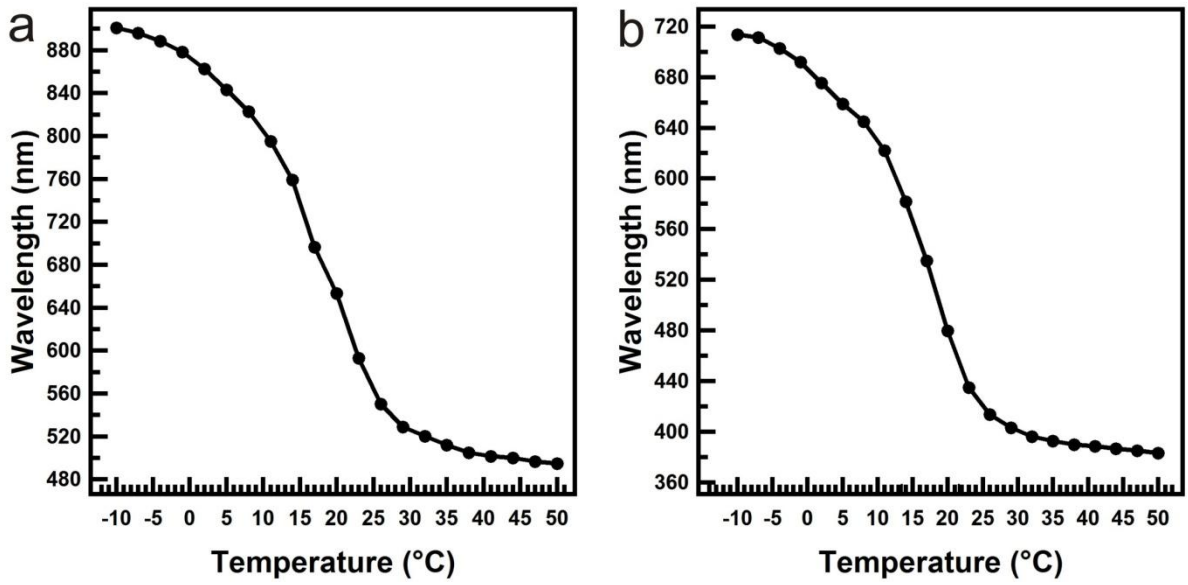

Figure 3-15. Plot of wavelength vs. temperature for a single peak in the reflectance spectrum of two etalons a and b as the temperature is increased in increments of 3 °C. The solvating solution is 20% methanol by volume.

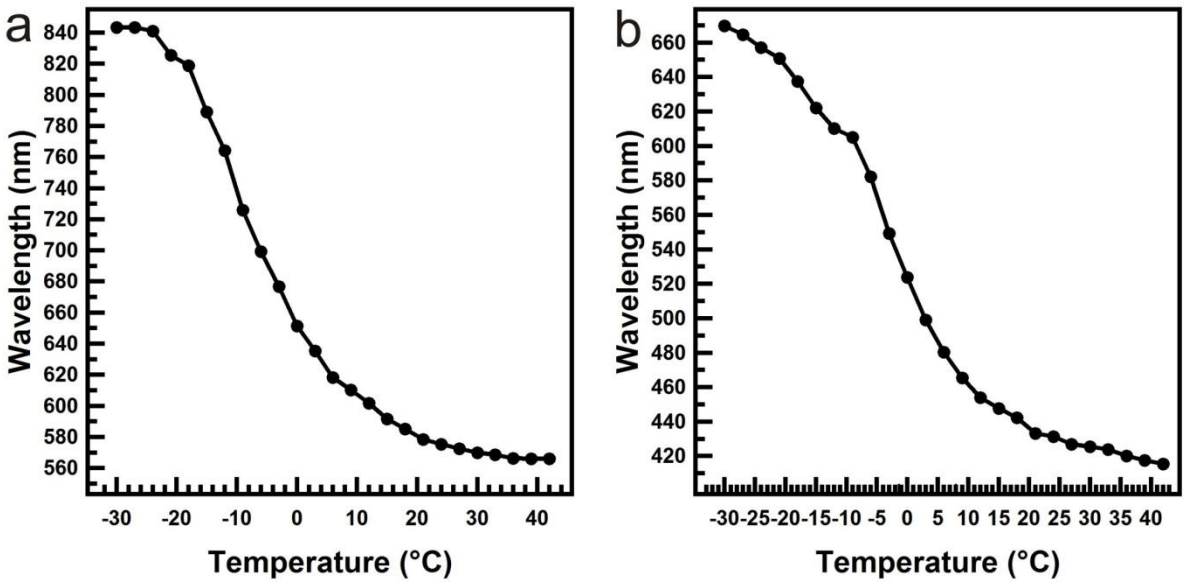

Figure 3-16. Plot of wavelength vs. temperature for a single peak in the reflectance spectrum of two etalons a and b as the temperature is increased in increments of 3 °C. The solvating solution is 40% methanol by volume.

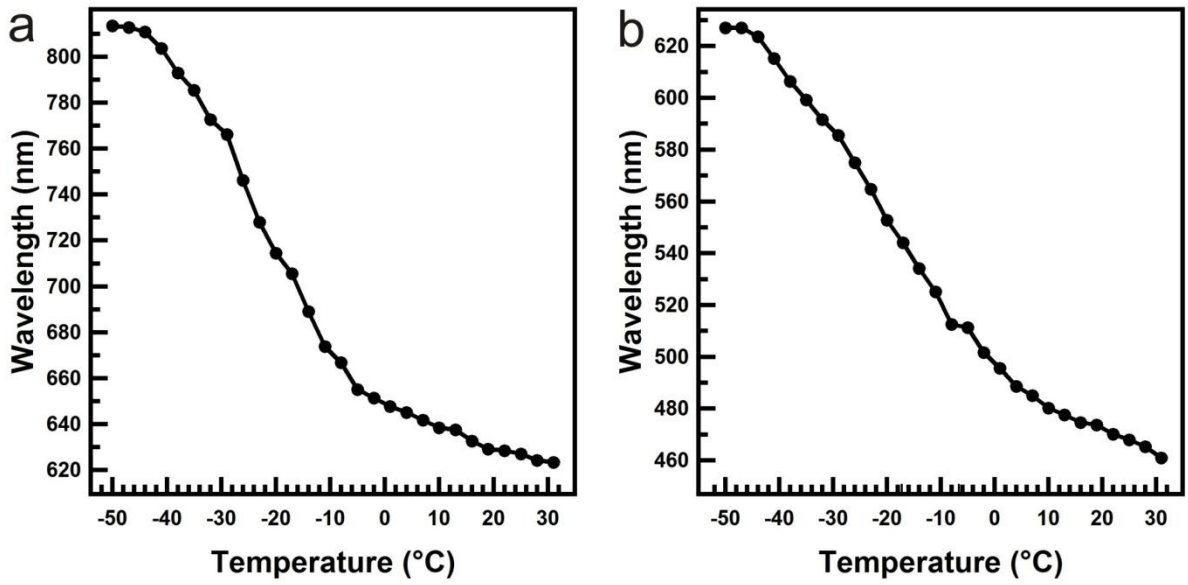

Figure 3-17. Plot of wavelength vs. temperature for a single peak in the reflectance spectrum of two etalons a and b as the temperature is increased in increments of 3 °C. The solvating solution is 55% methanol by volume.

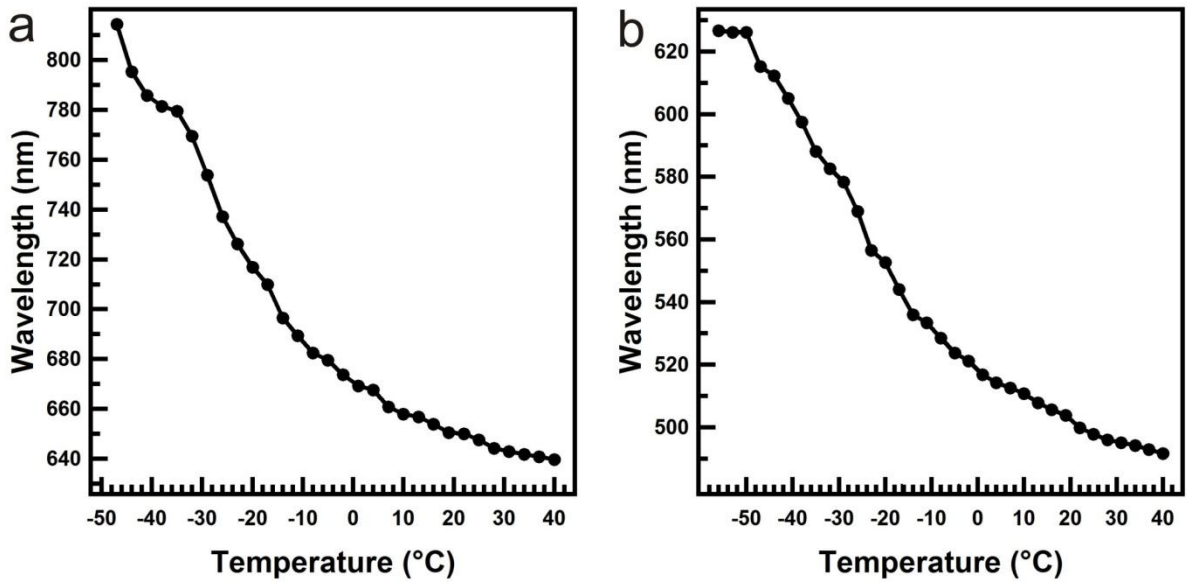

Figure 3-18. Plot of wavelength vs. temperature for a single peak in the reflectance spectrum of two etalons a and b as the temperature is increased in increments of 3 °C. The solvating solution is 60% methanol by volume.

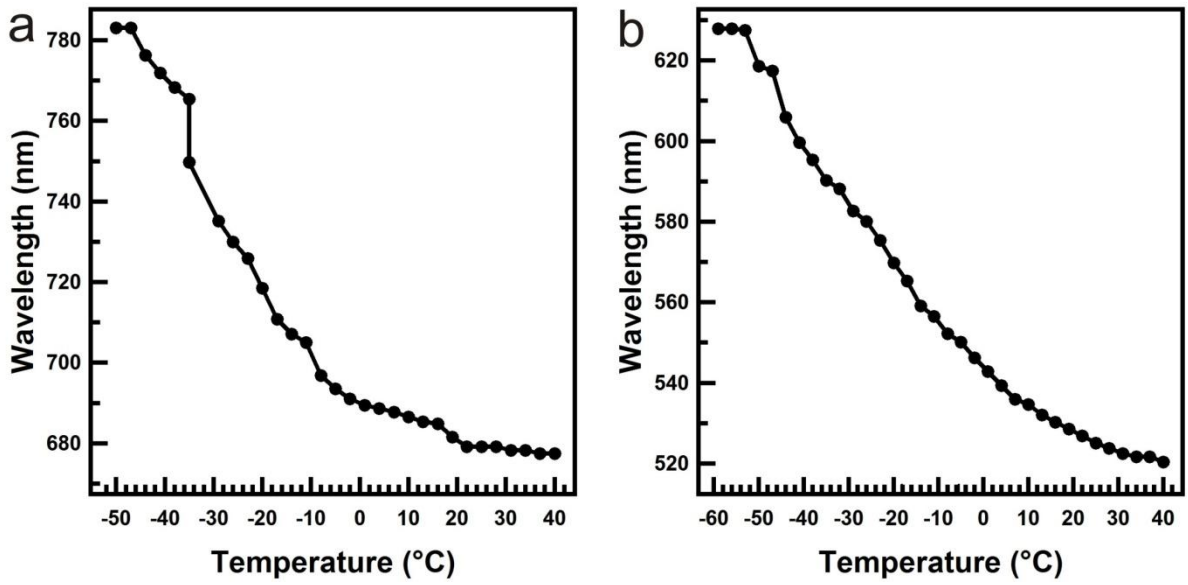

Figure 3-19. Plot of wavelength vs. temperature for a single peak in the reflectance spectrum of two etalons a and b as the temperature is increased in increments of 3 °C. The solvating solution is 65% methanol by volume.

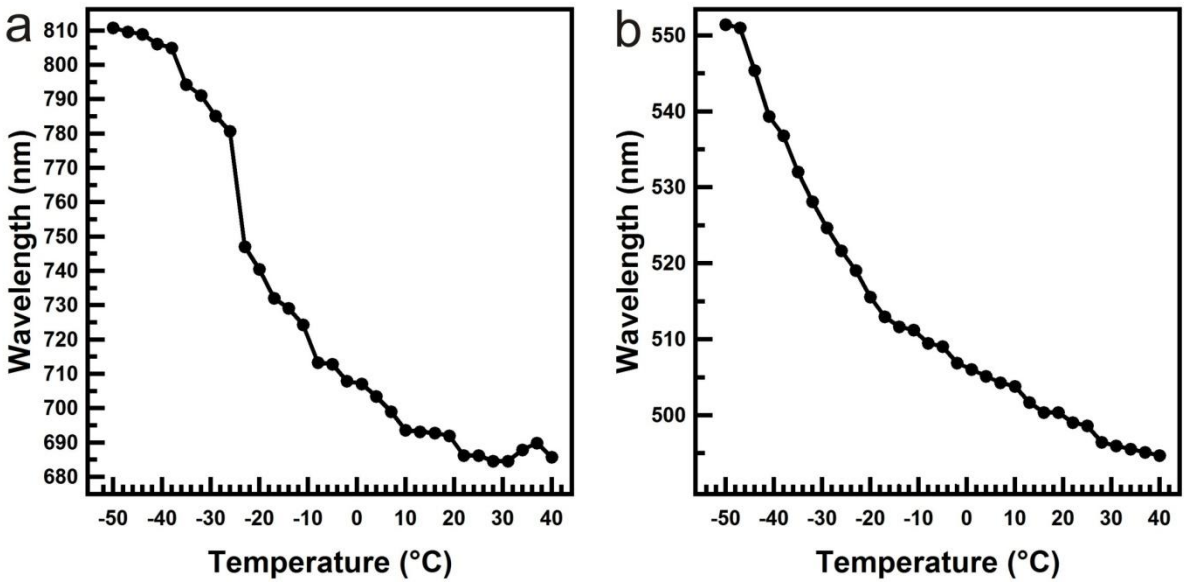

Figure 3-20. Plot of wavelength vs. temperature for a single peak in the reflectance spectrum of two etalons a and b as the temperature is increased in increments of 3 °C. The solvating solution is 70% methanol by volume.

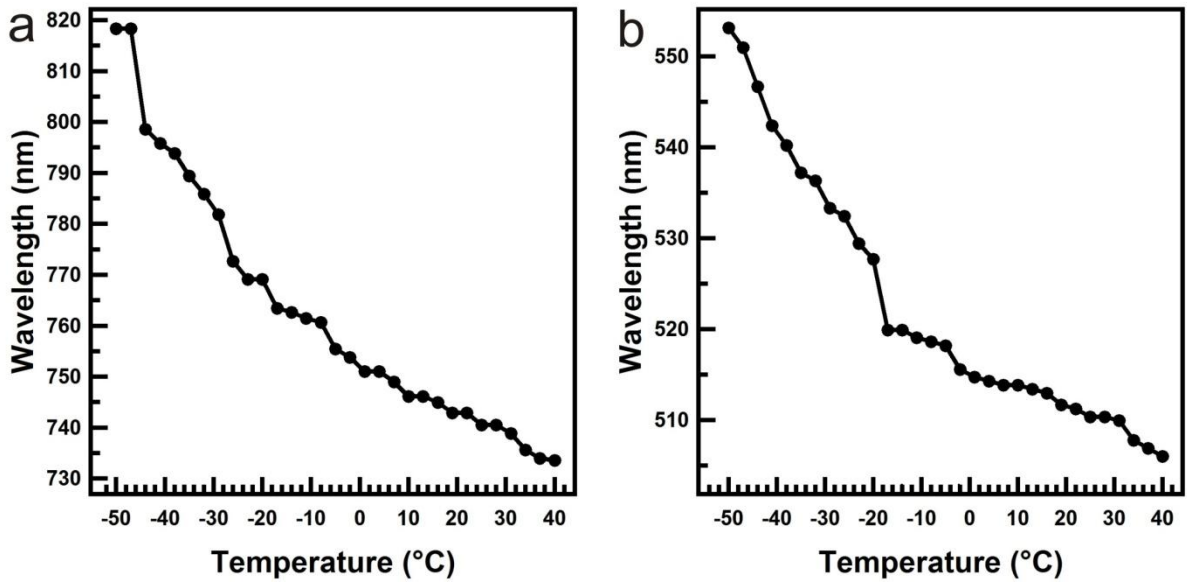

Figure 3-21. Plot of wavelength vs. temperature for a single peak in the reflectance spectrum of two etalons a and b as the temperature is increased in increments of 3 °C. The solvating solution is 75% methanol by volume.

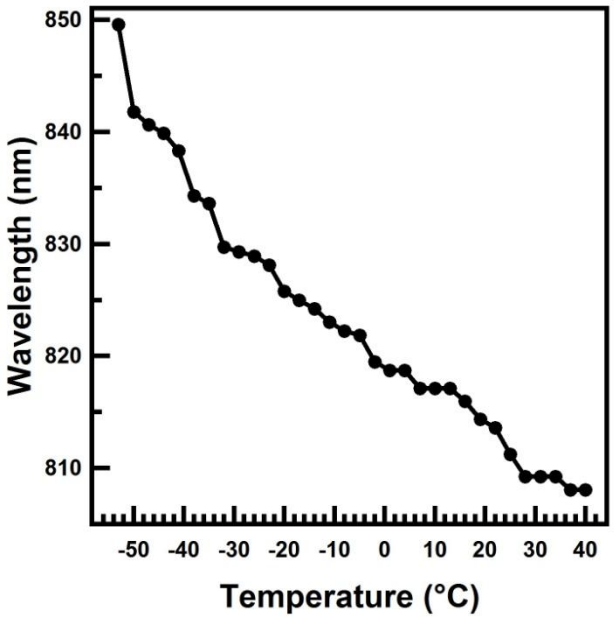

Figure 3-22. Plot of wavelength vs. temperature for a single peak in the reflectance spectrum of etalon as the temperature is increased in increments of 3 °C. The solvating solution is 80% methanol by volume.

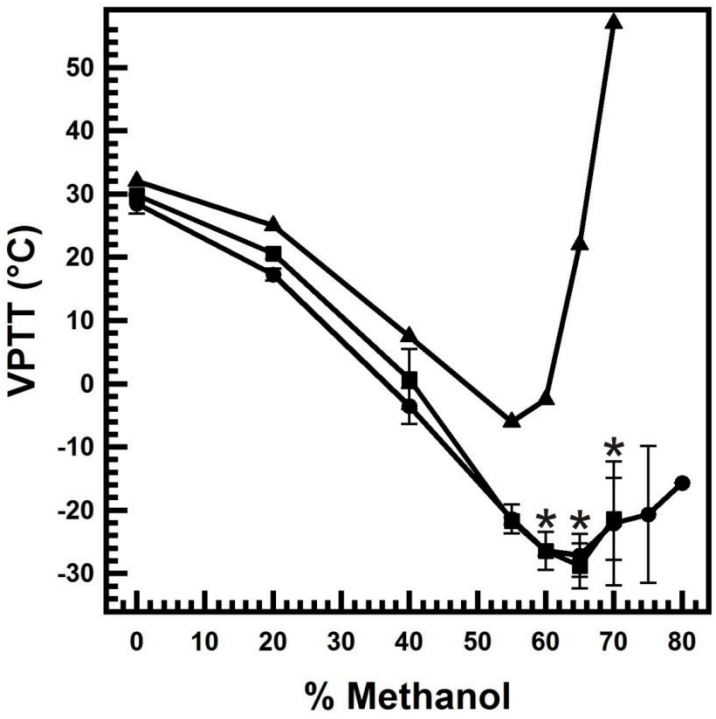

Figure 3-23. Plot of the average VPTT over a range of methanol concentration for microgels in an etalon (●) microgels in solution (■) and pNIPAm in literature (▲). The error bars being the standard deviation associated with each value[20] * Indicates approximated data for microgels in solution.

To confirm our findings, and to prevent MeOH from escaping the system during the experiment, which can affect the VPTT, we conducted the etalon experiments in a completely sealed chamber, the data for which can be seen in figure 3-24. For this experiment we used 70% (V/V) MeOH in water, and observed the shift in λ as a function of temperature; a VPTT of -26.6 °C was calculated for this experiment, which is well within the experimental error associated with the prior experiments, at -22.0 ±9.8 °C. Furthermore, Figure 3-25

shows that the magnitude of the signal change at the microgel's VPTT decreases as the MeOH concentration in the water increases, which is indicative that we are indeed exposing the microgel-based etalon to different MeOH concentrations. If this was not the case, we should not see the observed trends in Figure 3-25. We can also see this trend in figure 3-26, show all of the observed trends for one set of experiments

In addition to this, the position of a single peak of order m = 2 was observed at 25 °C as methanol was added to the system in 5% increments, then the reverse experiment was done by adding water to methanol in 5% increments to determine the reversibility. This data can be seen in Figures 3-27 to 3-29. The titration was repeated at low methanol concentrations in figure 3-28 to confirm the trend of a decreasing wavelength. The data show agreement with the previous experiments as the same overall trend is observed, not to mention that a shift is again observed as the methanol concentration is increased beyond 70% and still after even 80%.

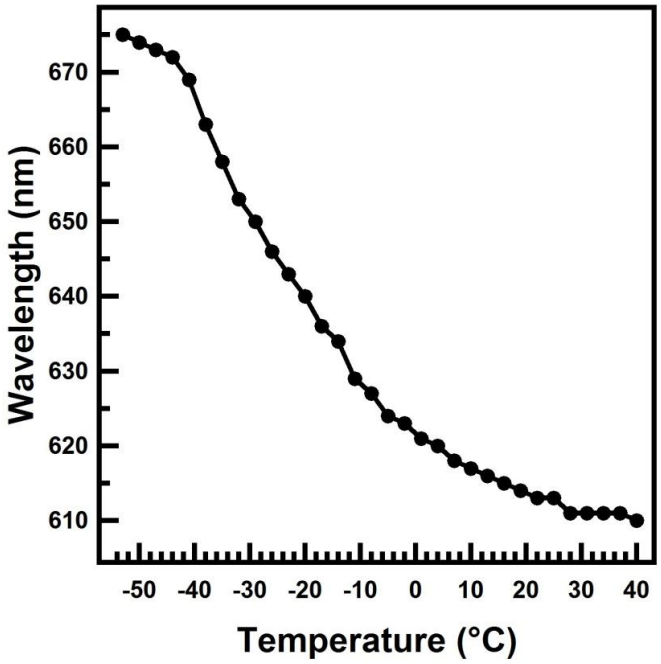

Figure 3-24. Plot of wavelength vs. temperature for a single peak in the reflectance spectrum of etalon in sealed environment as the temperature is increased in increments of 3 °C. The solvating solution is 70% methanol by volume.

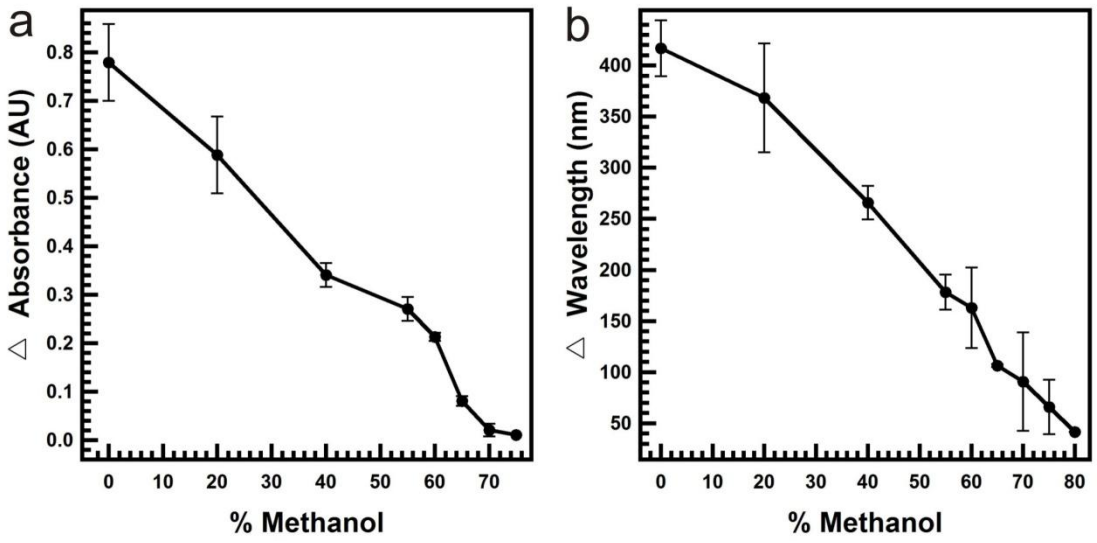

Figure 3-25. a) Plot of the average change in absorbance over VPTT of pNIPAm microgels in solution. b) Plot of the average change in wavelength over VPTT of pNIPAm microgel based etalons. The line being a guide and the error bars representing the standard deviation of the values.

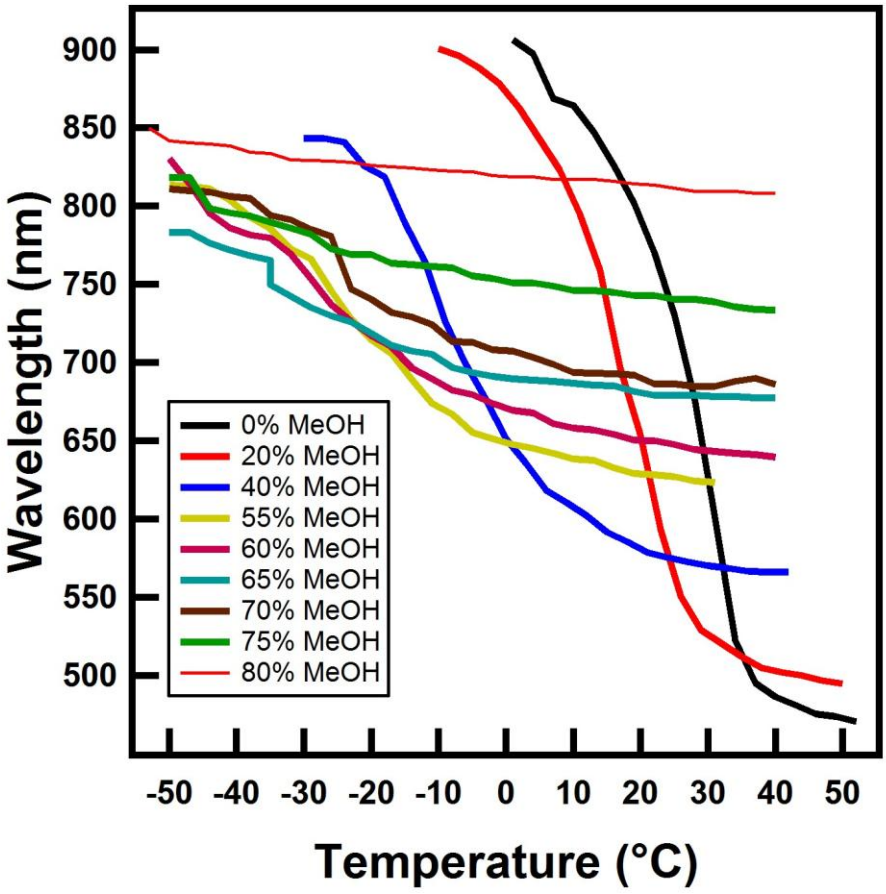

Figure 3-26. All collected data for microgels in an etalon in the first set of experiments.

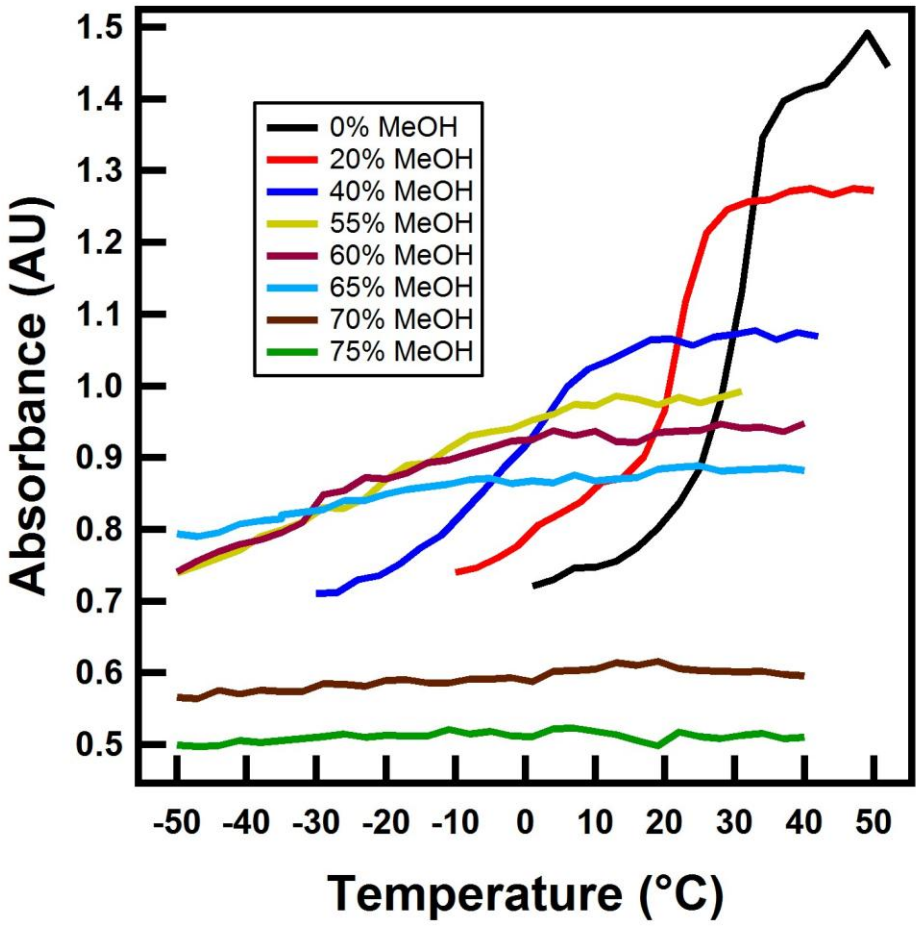

Figure 3-27. All collected data for microgels in solution in the first set of experiments.

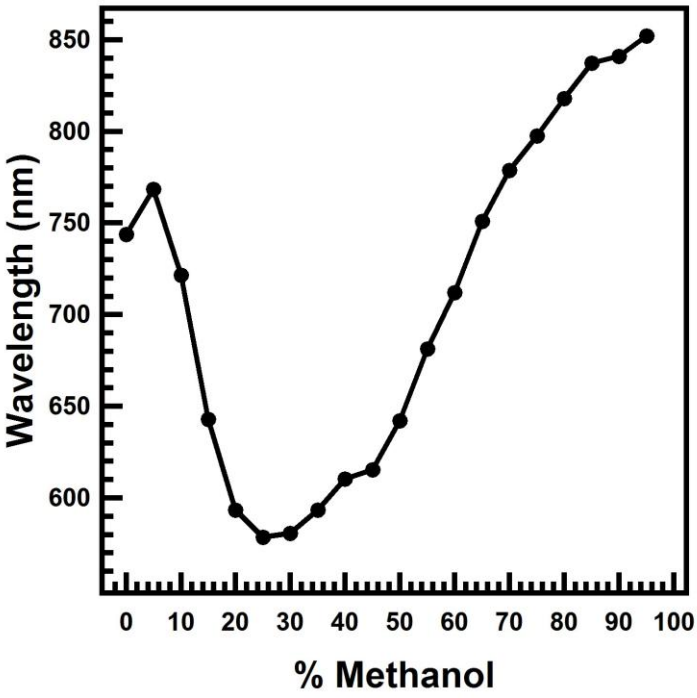

Figure 3-28. Plot of peak wavelength against concentration of methanol for pNIPAm microgel-based etalon in water at 25 °C as methanol is added increasing its concentration in 5 % increments.

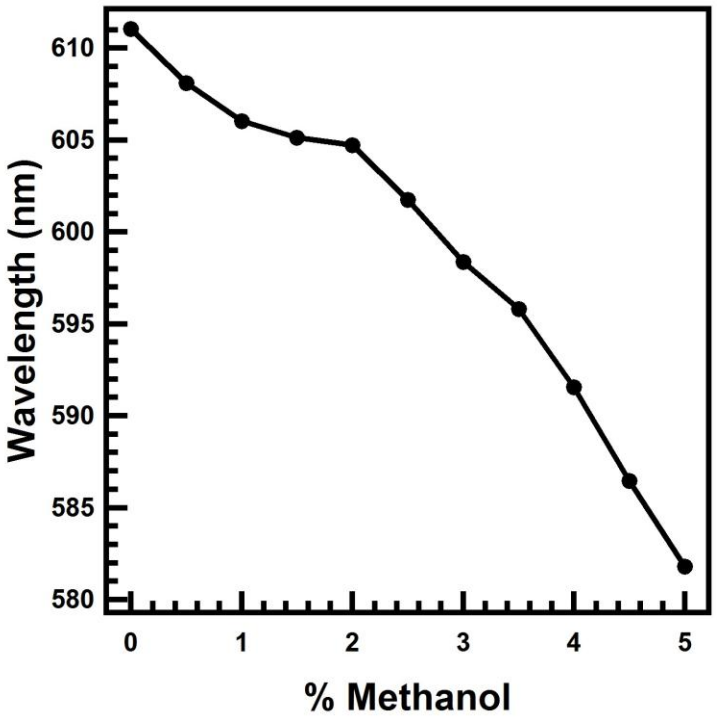

Figure 3-29. Plot of peak wavelength against concentration of methanol for pNIPAm microgel-based etalon in water at 25 °C as methanol is added increasing its concentration in 0.5 % increments for low concentrations.

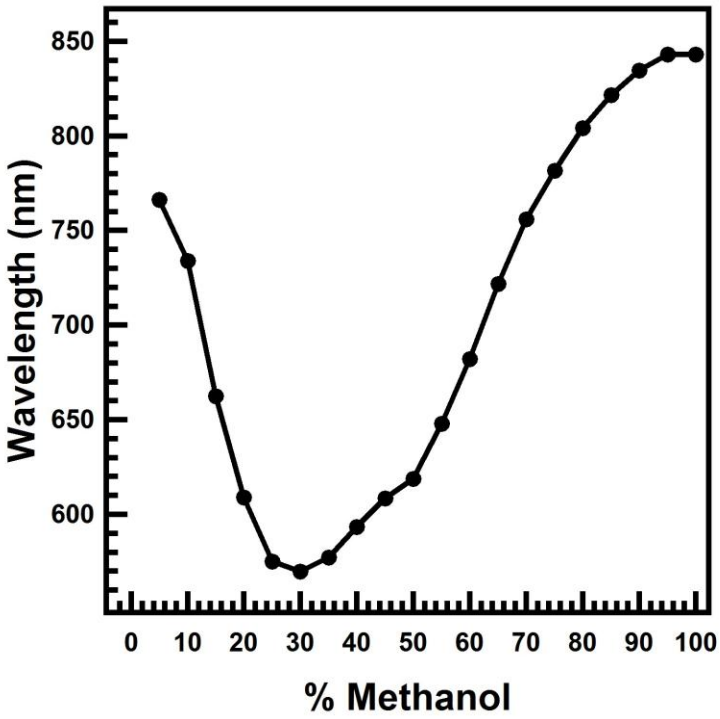

Figure 3-30. Plot of peak wavelength against concentration of methanol for pNIPAm microgel-based etalon in methanol at 25 °C as water is added, decreasing the methanol concentration in 5 % increments.

3.4. Conclusions

Relatively little is known about how confinement of pNIPAm-based microgels between surfaces affects their properties, e.g., their VPTT. In this study we showed that confinement does not drastically affect the VPTT of the pNIPAm-based microgels. We then used this to probe the behavior of microgels in various water/methanol solutions to determine pNIPAm-based microgel cononsolvency behavior. We were able to measure a VPTT for the pNIPAm-based microgels in aqueous solutions containing as much as 80% MeOH. Not only was the observed

VPTT for the pNIPAm-based microgels much lower than previously observed, a VPTT at such high MeOH concentrations has never been observed previously. We feel that this is a result of the pNIPAm microgel-based etalons allowing us to probe the microgels more carefully than has been previously possible.

Chapter 4

Conclusions and Future Work

4.1. Conclusions

Poly(*N*-isopropylacrylamide) (pNIPAm) microgel based etalons offer a new and unique device with a wide range of applications as a sensor. In order for these applications to be fully realised the devices must be fabricated in a consistent manner in such a way that allows for the fabrication of a large volume of the devices. In addition, in order to be considered as a point of care diagnostic device they need to be fabricated in such a way as to be available in remote areas that may not be able to afford complex devices made using expensive materials or complex fabrication methods. Finally, the properties of the device need to be explored further in order to have the fundamental understanding of the device necessary to continue developing not only the fabrication methods but new applications of the etalons.

In Chapter 2 the materials used for the semi-transparent reflective surfaces of the standard interferometer structure of the pNIPAm microgel based etalons was examined in the hopes of finding a new and cheaper material with which to fabricate the etalon and realise their potential in point of care diagnostics. It was determined that although Au gives reproducible etalons with homogenous reflectance spectra, other metals can produce the same results. The metals examined were Al, Cu, Ni, and Ti; all of which gave the same homogeneous microgel layer as devices fabricated using Au, confirmed by DIC microscopy. In

addition the devices fabricated using these alternate metals retained the same optical properties and temperature responsiveness that is well documented, although some minor differences in peak wavelength was seen and attributed to the natural difference in color of each metal.

In Chapter 3 the temperature at which the pNIPAm microgels collapse, the volume phase transition temperature (VPTT), was examined for the microgels both in solution and confined in an etalon device in order to gain an understanding of what effect, if any, confinement has on the properties of the microgels. It was determined that the confinement of the microgels had no affect on the VPTT, and from this it was determined that pNIPAm microgel based etalons were a valid way of determining the VPTT of pNIPAm based microgels. The VPTT was then determined in various methanol concentrations, giving significantly lower values than previously established for both linear pNIPAm and pNIPAm based microgels. In addition a transition was observed in methanol concentrations where there was previously thought to be no transition, possibly due to the unique method in used to examine the transition using an etalon device.

4.2. Future Work

The projects discussed here give rise to a better understanding; not only of the pNIPAm microgel based etalons and their fabrication, but also of the pNIPAm based microgels used to fabricate the devices. Additional experiments can now be

performed based on these results in order to continue developing the devices for diagnostics and to gain a better understanding of the etalons properties.

In Chapter 2 it was established that metals other than Au can be used to fabricate the pNIPAm microgel based etalons, and as such they can be made using cheaper materials. Now that this has been established it is possible to find an ideal material for the fabrication of the device, an ideal material having strong optical properties and that is robust enough to use in many environments. This can be done by fabricating the device with additional metals until an etalon is fabricated with ideal optical properties using a stable metal that will be able to resist any environment required in the day to day use of the device, while preferable remaining inexpensive to fabricate on a large scale. In addition it would be beneficial to examine alternate methods for the deposition of pNIPAm microgels on to the base metal layer in order to continue to develop the device with point of care diagnostics in mind.

In Chapter 3 the VPTTs of pNIPAm based microgels were found for a wide range of methanol concentrations and it was found that confinement of the microgels in an etalon did not have a measurable affect on the transition temperature. To expand on this data the procedure could be repeated using solvents other than methanol, for example ethanol or tetrahydafuran in which the transition temperatures have previously been established, to see if similar results are observed. Of particular interest would be if similar trends were observed, such as lower transition temperature than previously reported and possible detection of transitions at solvent concentrations not seen before. Another possible direction is

to modify the pNIPAm microgels with functional groups such as t-butyl, and observe what affect the additional hydrophobicity of the polymer will have on the transition temperature and if there is any deviation from previously established trends.

References

1. Papaphilippou, P. C.; Pourgouris, A.; Marinica, O.; Taculescu, A.; Athanasopoulos, G. I.; Vekas, L.; Krasia-Christoforou, T., Fabrication and characterization of superparamagnetic and thermoresponsive hydrogels based on oleic-acid-coated Fe3O4 nanoparticles, hexa(ethylene glycol) methyl ether methacrylate and 2-(acetoacetoxy)ethyl methacrylate. *J. Magn. Magn. Mater.* **2011,** 323, (5), 557-563.

2. Suzuki, A.; Tanaka, T., PHASE-TRANSITION IN POLYMER GELS INDUCED BY VISIBLE-LIGHT. *Nature* **1990,** 346, (6282), 345-347.

3. Swager, T. M.; Marsella, M. J., MOLECULAR RECOGNITION AND CHEMORESISTIVE MATERIALS. *Adv. Mater.* **1994,** 6, (7-8), 595-597.

4. Anderson, D. G.; Burdick, J. A.; Langer, R., Materials science - Smart biomaterials. *Science* **2004,** 305, (5692), 1923-1924.

5. Galaev, I. Y.; Mattiasson, B., 'Smart' polymers and what they could do in biotechnology and medicine. *Trends in Biotechnology* **1999,** 17, (8), 335-340.

6. Nagase, K.; Kobayashi, J.; Kikuchi, A.; Akiyama, Y.; Kanazawa, H.; Okano, T., Thermally-modulated on/off-adsorption materials for pharmaceutical protein purification. *Biomaterials* **2011,** 32, (2), 619-627.

7. Kumashiro, Y.; Ikezoe, Y.; Hayashi, T.; Okabayashi, Y.; Tamada, K.; Yamato, M.; Okano, T.; Hara, M., Temperature-modulated adsorption of poly(N-isopropylacrylamide)-grafted ferritin on solid substrate. *Colloid Surf. B-Biointerfaces* **2012,** 95, 57-64.

8. Schild, H. G.; Muthukumar, M.; Tirrell, D. A., CONONSOLVENCY IN MIXED AQUEOUS-SOLUTIONS OF POLY(N-ISOPROPYLACRYLAMIDE). *Macromolecules* **1991,** 24, (4), 948-952.

9. Schild, H. G., POLY (N-ISOPROPYLACRYLAMIDE) - EXPERIMENT, THEORY AND APPLICATION. *Prog. Polym. Sci.* **1992,** 17, (2), 163-249.

10. Kojima, H.; Tanaka, F.; Scherzinger, C.; Richtering, W., Temperature dependent phase behavior of PNIPAM microgels in mixed water/methanol solvents. *Journal of Polymer Science Part B: Polymer Physics* **2012**, n/a-n/a.

11. Shultz, A. R.; Flory, P. J., PHASE EQUILIBRIA IN POLYMER SOLVENT SYSTEMS. *J. Am. Chem. Soc.* **1952,** 74, (19), 4760-4767.

12. Wang, X. H.; Qiu, X. P.; Wu, C., Comparison of the coil-to-globule and the globule-to-coil transitions of a single poly(N-isopropylacrylamide) homopolymer chain in water. *Macromolecules* **1998,** 31, (9), 2972-2976.

13. Xu, J.; Zhu, Z. Y.; Luo, S. Z.; Wu, C.; Liu, S. Y., First observation of two-stage collapsing kinetics of a single synthetic polymer chain. *Phys. Rev. Lett.* **2006,** 96, (2).

14. Zhou, K. J.; Lu, Y. J.; Li, J. F.; Shen, L.; Zhang, G. Z.; Xie, Z. W.; Wu, C., The Coil-to-Globule-to-Coil Transition of Linear Polymer Chains in Dilute Aqueous Solutions: Effect of Intrachain Hydrogen Bonding. *Macromolecules* **2008,** 41, (22), 8927-8931.

15. Qiu, X. P.; Koga, T.; Tanaka, F.; Winnik, F. M., New insights into the effects of molecular weight and end group on the temperature-induced phase transition of poly(N-isopropylacrylamide) in water. *Sci. China-Chem.* **2013,** 56, (1), 56-64.

16. Blackburn, W. H.; Lyon, L. A., Size-controlled synthesis of monodisperse core/shell nanogels. *Colloid Polym. Sci.* **2008,** 286, (5), 563-569.

17. Brazel, C. S.; Peppas, N. A., SYNTHESIS AND CHARACTERIZATION OF THERMOMECHANICALLY AND CHEMOMECHANICALLY RESPONSIVE POLY(N-ISOPROPYLACRYLAMIDE-CO-METHACRYLIC ACID) HYDROGELS. *Macromolecules* **1995,** 28, (24), 8016-8020.

18. Gutowska, A.; Bae, Y. H.; Jacobs, H.; Feijen, J.; Kim, S. W., THERMOSENSITIVE INTERPENETRATING POLYMER NETWORKS - SYNTHESIS, CHARACTERIZATION, AND MACROMOLECULAR RELEASE. *Macromolecules* **1994,** 27, (15), 4167-4175.

19. Jones, C. D.; Lyon, L. A., Synthesis and characterization of multiresponsive core-shell microgels. *Macromolecules* **2000,** 33, (22), 8301-8306.

20. Meng, Z. Y.; Smith, M. H.; Lyon, L. A., Temperature-programmed synthesis of micron-sized multi-responsive microgels. *Colloid Polym. Sci.* **2009,** 287, (3), 277-285.

21. Debord, J. D.; Lyon, L. A., Thermoresponsive photonic crystals. *J. Phys. Chem. B* **2000,** 104, (27), 6327-6331.

22. Gan, D. J.; Lyon, L. A., Tunable swelling kinetics in core-shell hydrogel nanoparticles. *J. Am. Chem. Soc.* **2001,** 123, (31), 7511-7517.

23. Hoare, T.; Pelton, R., Highly pH and temperature responsive microgels functionalized with vinylacetic acid. *Macromolecules* **2004,** 37, (7), 2544-2550.

24. Kim, J.; Serpe, M. J.; Lyon, L. A., Hydrogel microparticles as dynamically tunable microlenses. *J. Am. Chem. Soc.* **2004,** 126, (31), 9512-9513.

25. Lyon, L. A.; Debord, J. D.; Debord, S. B.; Jones, C. D.; McGrath, J. G.; Serpe, M. J., Microgel colloidal crystals. *J. Phys. Chem. B* **2004,** 108, (50), 19099-19108.

26. Parasuraman, D.; Serpe, M. J., Poly (N-Isopropylacrylamide) Microgel-Based Assemblies for Organic Dye Removal from Water. *ACS Appl. Mater. Interfaces* **2011,** 3, (12), 4714-4721.

27. Parasuraman, D.; Serpe, M. J., Poly (N-Isopropylacrylamide) Microgels for Organic Dye Removal from Water. *ACS Appl. Mater. Interfaces* **2011,** 3, (7), 2732-2737.

28. Pelton, R. H.; Chibante, P., PREPARATION OF AQUEOUS LATTICES WITH N-ISOPROPYLACRYLAMIDE. *Colloids and Surfaces* **1986,** 20, (3), 247-256.

29. Snowden, M. J.; Chowdhry, B. Z.; Vincent, B.; Morris, G. E., Colloidal copolymer microgels of N-isopropylacrylamide and acrylic acid: pH, ionic strength and temperature effects. *J. Chem. Soc.-Faraday Trans.* **1996,** 92, (24), 5013-5016.

30. Suzuki, D.; Kawaguchi, H., Stimuli-sensitive core/shell template particles for immobilizing inorganic nanoparticles in the core. *Colloid Polym. Sci.* **2006,** 284, (12), 1443-1451.

31. Suzuki, D.; McGrath, J. G.; Kawaguchi, H.; Lyon, L. A., Colloidal crystals of thermosensitive, core/shell hybrid microgels. *J. Phys. Chem. C* **2007,** 111, (15), 5667-5672.

32. Tsuji, S.; Kawaguchi, H., Colored thin films prepared from hydrogel microspheres. *Langmuir* **2005,** 21, (18), 8439-8442.

33. Alexeev, V. L.; Sharma, A. C.; Goponenko, A. V.; Das, S.; Lednev, I. K.; Wilcox, C. S.; Finegold, D. N.; Asher, S. A., High ionic strength glucose-sensing photonic crystal. *Anal. Chem.* **2003,** 75, (10), 2316-2323.

34. Bonanno, L. M.; DeLouise, L. A., Integration of a Chemical-Responsive Hydrogel into a Porous Silicon Photonic Sensor for Visual Colorimetric Readout. *Adv. Funct. Mater.* **2010,** 20, (4), 573-578.

35. Hoare, T.; Pelton, R., Engineering glucose swelling responses in poly(N-isopropylacrylamide)-based microgels. *Macromolecules* **2007,** 40, (3), 670-678.

36. Kim, J.; Nayak, S.; Lyon, L. A., Bioresponsive hydrogel microlenses. *J. Am. Chem. Soc.* **2005,** 127, (26), 9588-9592.

37. Kim, J. S.; Singh, N.; Lyon, L. A., Label-free biosensing with hydrogel microlenses. *Angew. Chem.-Int. Edit.* **2006,** 45, (9), 1446-1449.

38. Pelton, R., Temperature-sensitive aqueous microgels. *Adv. Colloid Interface Sci.* **2000,** 85, (1), 1-33.

39. Wu, C., A comparison between the 'coil-to-globule' transition of linear chains and the "volume phase transition" of spherical microgels. *Polymer* **1998,** 39, (19), 4609-4619.

40. Winnik, F. M.; Ottaviani, M. F.; Bossmann, S. H.; Garciagaribay, M.; Turro, N. J., CONONSOLVENCY OF POLY(N-ISOPROPYLACRYLAMIDE) IN MIXED WATER-METHANOL SOLUTIONS - A LOOK AT SPIN-LABELED POLYMERS. *Macromolecules* **1992,** 25, (22), 6007-6017.

41. Winnik, F. M.; Ringsdorf, H.; Venzmer, J., METHANOL WATER AS A CO-NONSOLVENT SYSTEM FOR POLY(N-ISOPROPYLACRYLAMIDE). *Macromolecules* **1990,** 23, (8), 2415-2416.

42. Sorrell, C. D.; Carter, M. C. D.; Serpe, M. J., Color Tunable Poly (N-Isopropylacrylamide)-co-Acrylic Acid Microgel-Au Hybrid Assemblies. *Adv. Funct. Mater.* **2011,** 21, (3), 425-433.

43. Sorrell, C. D.; Serpe, M. J., Reflection Order Selectivity of Color-Tunable Poly(N-isopropylacrylamide) Microgel Based Etalons. *Adv. Mater.* **2011,** 23, (35), 4088-+.

44. Sorrell, C. D.; Carter, M. C. D.; Serpe, M. J., A "Paint-On" Protocol for the Facile Assembly of Uniform Microgel Coatings for Color Tunable Etalon Fabrication. *ACS Appl. Mater. Interfaces* **2011,** 3, (4), 1140-1147.

45. Brooker, G., *Modern classical optics*. Oxford University Press: Oxford, 2003; p 397.

46. Hariharan, P., *Basics of interferometry*. Academic Press: Burlington, 2007; p 226.

47. Sorrell, C. D.; Serpe, M. J., Glucose sensitive poly (N-isopropylacrylamide) microgel based etalons. *Anal. Bioanal. Chem.* **2012,** 402, (7), 2385-2393.

48. Hu, L.; Serpe, M. J., Color modulation of spatially isolated regions on a single poly(N-isopropylacrylamide) microgel based etalon. *J. Mater. Chem.* **2012,** 22, (17), 8199-8202.

49. Johnson, K. C. C.; Mendez, F.; Serpe, M. J., Detecting solution pH changes using poly (N-isopropylacrylamide)-co-acrylic acid microgel-based etalon modified quartz crystal microbalances. *Anal. Chim. Acta* **2012,** 739, 83-88.

50. Islam, M. R.; Serpe, M. J., Penetration of Polyelectrolytes into Charged Poly(N-isopropylacrylamide) Microgel Layers Confined between Two Surfaces. *Macromolecules* **2013,** 46, (4), 1599-1606.

51. Islam, M. R.; Serpe, M. J., Polyelectrolyte mediated intra and intermolecular crosslinking in microgel-based etalons for sensing protein concentration in solution. *Chem. Commun.* **2013,** 49, (26), 2646-2648.

52. Yager, P.; Domingo, G. J.; Gerdes, J., Point-of-care diagnostics for global health. In *Annual Review of Biomedical Engineering*, 2008; Vol. 10, pp 107-144.

53. Heppner, I.; Serpe, M., Poly (N-isopropylacrylamide) microgel-based etalons constructed from various metal layers. *Colloid Polym. Sci.* **2013**, 1-6.

54. Baca, J. T.; Finegold, D. N.; Asher, S. A., Progress in developing polymerized crystalline colloidal array sensors for point-of-care detection of myocardial ischemia. *Analyst* **2008,** 133, (3), 385-390.

55. Carter, M. C. D.; Sorrell, C. D.; Serpe, M. J., Deswelling Kinetics of Color Tunable Poly(N-Isopropylacrylamide) Microgel-Based Etalons. *J. Phys. Chem. B* **2011,** 115, (49), 14359-14368.

56. Holtz, J. H.; Asher, S. A., Polymerized colloidal crystal hydrogel films as intelligent chemical sensing materials. *Nature* **1997,** 389, (6653), 829-832.

57. Kang, Y.; Walish, J. J.; Gorishnyy, T.; Thomas, E. L., Broad-wavelength-range chemically tunable block-copolymer photonic gels. *Nat. Mater.* **2007,** 6, (12), 957-960.

58. Kimble, K. W.; Walker, J. P.; Finegold, D. N.; Asher, S. A., Progress toward the development of a point-of-care photonic crystal ammonia sensor. *Anal. Bioanal. Chem.* **2006,** 385, (4), 678-685.

59. Mabey, D.; Peeling, R. W.; Ustianowski, A.; Perkins, M. D., Diagnostics for the developing world. *Nat. Rev. Microbiol.* **2004,** 2, (3), 231-240.

60. Tudos, A. J.; Besselink, G. A. J.; Schasfoort, R. B. M., Trends in miniaturized total analysis systems for point-of-care testing in clinical chemistry. *Lab Chip* **2001,** 1, (2), 83-95.

61. Alexeev, V. L.; Das, S.; Finegold, D. N.; Asher, S. A., Photonic crystal glucose-sensing material for noninvasive monitoring of glucose in tear fluid. *Clin. Chem.* **2004,** 50, (12), 2353-2360.

62. Ben-Moshe, M.; Alexeev, V. L.; Asher, S. A., Fast responsive crystalline colloidal array photonic crystal glucose sensors. *Anal. Chem.* **2006,** 78, (14), 5149-5157.

63. Holtz, J. H.; Holtz, J. S. W.; Munro, C. H.; Asher, S. A., Intelligent polymerized crystalline colloidal arrays: Novel chemical sensor materials. *Anal. Chem.* **1998,** 70, (4), 780-791.

64. Muscatello, M. M. W.; Stunja, L. E.; Asher, S. A., Polymerized Crystalline Colloidal Array Sensing of High Glucose Concentrations. *Anal. Chem.* **2009,** 81, (12), 4978-4986.

65. Alfrey, T.; Bradford, E. B.; Vanderhoff, J. W.; Oster, G., OPTICAL PROPERTIES OF UNIFORM PARTICLE-SIZE LATEXES. *Journal of the Optical Society of America* **1954,** 44, (8), 603-609.

66. Figotin, A.; Godin, Y. A.; Vitebsky, I., Two-dimensional tunable photonic crystals. *Phys. Rev. B* **1998,** 57, (5), 2841-2848.

67. Lotsch, B. V.; Ozin, G. A., Clay Bragg Stack Optical Sensors. *Adv. Mater.* **2008,** 20, (21), 4079-+.

68. Sanders, J. V., DIFFRACTION OF LIGHT BY OPALS. *Acta Crystallographica Section a-Crystal Physics Diffraction Theoretical and General Crystallography* **1968,** A 24, 427-&.

69. Crowther, H. M.; Vincent, B., Swelling behavior of poly N-isopropylacrylamide microgel particles in alcoholic solutions. *Colloid Polym. Sci.* **1998,** 276, (1), 46-51.

70. Kawaguchi, H., Functions of monodisperse, thermosensitive hydrogel microspheres. In *Biomedical Functions and Biotechnology of Natural and Artificial Polymers: Self-Assemblies, Hybrid Complexes and Biological Conjugates of Glycans, Liposomes, Polyethylene Glycols, Polyisopropylacrylamides, and Polypeptides*, Yalpani, M., Ed. 1996; Vol. 3, pp 157-168.

71. Kratz, K.; Eimer, W., Swelling properties of colloidal poly(N-isopropylacrylamide) microgels in solution. *Ber. Bunsen-Ges. Phys. Chem. Chem. Phys.* **1998,** 102, (6), 848-854.

72. Wu, C.; Zhou, S. Q.; Auyeung, S. C. F.; Jiang, S. H., Volume phase transition of spherical microgel particles. *Angew. Makromol. Chem.* **1996,** 240, 123-136.

73. Du, H. B.; Wickramasinghe, R.; Qian, X. H., Effects of Salt on the Lower Critical Solution Temperature of Poly (N-Isopropylacrylamide). *J. Phys. Chem. B* **2010,** 114, (49), 16594-16604.

74. Furyk, S.; Zhang, Y. J.; Ortiz-Acosta, D.; Cremer, P. S.; Bergbreiter, D. E., Effects of end group polarity and molecular weight on the lower critical

solution temperature of poly(N-isopropylacrylamide). *J. Polym. Sci. Pol. Chem.* **2006,** 44, (4), 1492-1501.

75. Gong, X. J.; Wu, C.; Ngai, T., Surface interaction forces mediated by poly(N-isopropylacrylamide) (PNIPAM) polymers: effects of concentration and temperature. *Colloid Polym. Sci.* **2010,** 288, (10-11), 1167-1172.

76. Sun, S. T.; Wu, P. Y., Role of Water/Methanol Clustering Dynamics on Thermosensitivity of Poly(N-isopropylacrylamide) from Spectral and Calorimetric Insights. *Macromolecules* **2010,** 43, (22), 9501-9510.

77. Walter, J.; Sehrt, J.; Vrabec, J.; Hasse, H., Molecular Dynamics and Experimental Study of Conformation Change of Poly(N-isopropylacrylamide) Hydrogels in Mixtures of Water and Methanol. *J. Phys. Chem. B* **2012,** 116, (17), 5251-5259.

78. Yamauchi, H.; Maeda, Y., LCST and UCST Behavior of Poly(N-isopropylacrylamide) in DMSO Water mixed solvents studied by IR and micro-raman Spectroscopy. *J. Phys. Chem. B* **2007,** 111, (45), 12964-12968.

79. Zhang, Y.; Furyk, S.; Sagle, L. B.; Cho, Y.; Bergbreiter, D. E.; Cremer, P. S., Effects of Hofmeister anions on the LCST of PNIPAM as a function of molecular weight. *J. Phys. Chem. C* **2007,** 111, (25), 8916-8924.

80. Chee, C. K.; Hunt, B. J.; Rimmer, S.; Soutar, I.; Swanson, L., Time-resolved fluorescence anisotropy studies of the cononsolvency of poly(N-isopropyl acrylamide) in mixtures of methanol and water. *Soft Matter* **2011,** 7, (3), 1176-1184.

81. Hao, J. K.; Cheng, H.; Butler, P.; Zhang, L.; Han, C. C., Origin of cononsolvency, based on the structure of tetrahydrofuran-water mixture. *J. Chem. Phys.* **2010,** 132, (15).

82. Pagonis, K.; Bokias, G., Upper critical solution temperature-type cononsolvency of poly(N,N-dimethylacrylamide) in water-organic solvent mixtures. *Polymer* **2004,** 45, (7), 2149-2153.

83. Scherzinger, C.; Holderer, O.; Richter, D.; Richtering, W., Polymer dynamics in responsive microgels: influence of cononsolvency and microgel architecture. *Phys. Chem. Chem. Phys.* **2012,** 14, (8), 2762-2768.

84. Sui, X. F.; Chen, Q.; Hempenius, M. A.; Vancso, G. J., Probing the Collapse Dynamics of Poly(N-isopropylacrylamide) Brushes by AFM: Effects of Co-nonsolvency and Grafting Densities. *Small* **2011,** 7, (10), 1440-1447.

85. Tanaka, F.; Koga, T.; Kojima, H.; Xue, N.; Winnik, F. M., Preferential Adsorption and Co-nonsolvency of Thermoresponsive Polymers in Mixed Solvents of Water/Methanol. *Macromolecules* **2011,** 44, (8), 2978-2989.

86. Tanaka, F.; Koga, T.; Winnik, F. M., Competitive Hydrogen Bonds and Cononsolvency of Poly(N-isopropylacrylamide)s in Mixed Solvents of Water/Methanol. In *Gels: Structures, Properties, and Functions: Fundamentals and Applications*, Tokita, M.; Nishinari, K., Eds. 2009; Vol. 136, pp 1-7.

87. Anac, I.; Aulasevich, A.; Junk, M. J. N.; Jakubowicz, P.; Roskamp, R. F.; Menges, B.; Jonas, U.; Knoll, W., Optical Characterization of Co-Nonsolvency Effects in Thin Responsive PNIPAAm-Based Gel Layers Exposed to Ethanol/Water Mixtures. *Macromol. Chem. Phys.* **2010,** 211, (9), 1018-1025.